

T-4278

APPLICATION OF A HIGH PRESSURE
WATER JET FOR TRONA CUTTING

ARTHUR LAKES LIBRARY
COLORADO SCHOOL OF MINES
GOLDEN, CO 80401

by
Eric J. White

ProQuest Number: 10783853

All rights reserved

INFORMATION TO ALL USERS

The quality of this reproduction is dependent upon the quality of the copy submitted.

In the unlikely event that the author did not send a complete manuscript and there are missing pages, these will be noted. Also, if material had to be removed, a note will indicate the deletion.



ProQuest 10783853

Published by ProQuest LLC (2018). Copyright of the Dissertation is held by the Author.

All rights reserved.

This work is protected against unauthorized copying under Title 17, United States Code
Microform Edition © ProQuest LLC.

ProQuest LLC.
789 East Eisenhower Parkway
P.O. Box 1346
Ann Arbor, MI 48106 – 1346


T-4278

A Thesis Submitted to the faculty and Board of Trustees of the Colorado School of Mines in partial fulfillment of the requirements for the degree of Master of Science (Mining Engineering).

Golden, Colorado

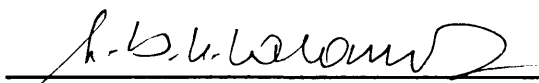
Date March 21, 1993

Signed: 
Eric J. White

Approved: 
Dr. Fun-Den Wang
Thesis Advisor

Golden, Colorado

Date April 1, 1993


for Dr. Donald W. Gentry
Professor and Head,
Department of
Mining Engineering

ABSTRACT

An overview of the technology of water jet cutting in the field of mining is presented. The application of using a high pressure water jet for the cutting of trona, a sodium carbonate solid found in Southwest Wyoming, is included. The purpose of the research is to identify the parameters of water jet cutting which affect the rate of removal, to test these parameters, and to find the range of cutting performance which displays the best rate of cutting, at the lowest specific energy.

The pump utilized in the research was manufactured by Haskel, Inc. It is an eight horsepower pneumatically-driven intensifier pump capable of producing a water jet with pressures up to 35,000 psi. at volumes under 1 gpm.

Parameters tested were: the nozzle size, the traverse velocity of the jet across the sample, the stand off distance between the nozzle and the target surface, the directional properties of the sample with respect to the jet direction of flow, and the relationship between the optimal jet pressure and volumetric flow. The nozzle sizes tested were 0.011 inches, 0.013 inches, 0.016 inches, and 0.019 inches. The traverse velocities tested were two in/sec., six in/sec., 12 in/sec., and 20 in/sec. The pressure ranges tested were different for each nozzle, since each nozzle size performs in a unique range of pressures. These pressure ranges were 6,500 to 13,700 psi. for the 0.019 inch nozzle, 8,700 to 15,300 psi. for the 0.016 inch nozzle, 13,300 to 24,800 psi. for the 0.013 inch nozzle, and 14,600 to 34,600 psi. for the 0.011 inch nozzle.

It was found that the best results of cutting performance were obtained when using the smaller nozzle sizes. The 0.011 inch nozzle produced a cutting rate of over 6.4 cubic centimeters per second, at a traverse velocity of 12 inches per second and a pressure of 23,500 psi. The 0.013 inch nozzle produced a cutting rate of over 7.1 cubic centimeters per second, at a traverse velocity of 12 inches per second and a pressure of 24,800 psi. The 0.016 inch nozzle produced a cutting rate over 6.2 cubic centimeters per second, at a traverse velocity of 12 inches per second and a pressure of 15,300 psi., and the 0.019 inch nozzle produced a cutting rate over 3.4 cubic centimeters per second, at a traverse velocity of six inches per second and a pressure of 13,700 psi.

Specific energy of cutting tended to decrease with an increase of pressure over all ranges of nozzle sizes. The specific energy was also found to decrease up to a traverse velocity of 12 inches per second, and then increase at traverse velocities higher than this.

It was concluded that trona can be effectively cut with a water jet. Other parameters which are not addressed in the scope of this thesis involve the kerf spacing, and the effect of cutting trona using higher pressures and volumes than those obtained by the equipment tested.

TABLE OF CONTENTS

| | Page |
|--|------|
| ABSTRACT | iii |
| LIST OF FIGURES | viii |
| LIST OF GRAPHS | ix |
| LIST OF TABLES | xi |
| ACKNOWLEDGMENTS | xii |
| DEDICATION | xiii |
| INTRODUCTION | 1 |
| CHAPTER 1. HISTORY | 3 |
| 1.1 History of Mining Using Water Jets. | 3 |
| 1.2 Description of Early Monitors | 5 |
| 1.3 Growth of Monitor Technology Underground. | 5 |
| 1.4 Water Jet Assisted Mechanical Mining. | 7 |
| 1.5 Mining Methods Utilizing Hydraulic Mining | 8 |
| CHAPTER 2. HIGH PRESSURE PUMPS AND TYPES OF JETS | 11 |
| 2.1 High Pressure Pumps | 11 |
| 2.2 Types of Jets | 13 |
| 2.2.1 Continuous Jets. | 13 |
| 2.2.2 Pulsed Jets | 14 |
| 2.2.3 Cavitating Jets | 15 |
| CHAPTER 3. FLUID DYNAMICS OF WATER JETS | 16 |
| CHAPTER 4. WATER JET ROCK CUTTING | 25 |
| CHAPTER 5. STATEMENT OF THESIS INTENT | 30 |
| 5.1 Objective of Thesis | 30 |
| 5.2 Approach to Thesis Objective | 30 |
| 5.2.1 Equipment Set Up | 31 |
| 5.2.2 Parameters Applying to Research | 32 |
| 5.3 Scope of the Research | 33 |
| CHAPTER 6. WATER JET PARAMETERS | 35 |

| | | |
|---|---|----|
| 6.1 | Pressure-to-Volume Ratio | 35 |
| 6.2 | Nozzle Size | 36 |
| 6.3 | Stand-Off Distance | 41 |
| 6.4 | Traverse Velocity | 42 |
| 6.5 | Effect of Materials Directional Property. | 43 |
| 6.6 | Other Parameters Which are Not Addressed. | 44 |
| CHAPTER 7. EXPERIMENTAL EQUIPMENT DESCRIPTION . . | | 45 |
| 7.1 | Pneumatic Intensifier Pump | 45 |
| 7.1.1 | Scope of the Intensifier Pump. . . | 45 |
| 7.2 | High Pressure Connections | 47 |
| 7.3 | Nozzle Configuration and Design | 47 |
| 7.4 | Feed Pump | 48 |
| 7.5 | Air Filter Unit | 48 |
| 7.6 | Water Filter Unit | 48 |
| 7.7 | Rodless Cylinder Traverse Mechanism . . . | 49 |
| 7.8 | Sample Support on Cylinder. | 49 |
| 7.9 | Traverse Velocity Instrumentation | 49 |
| 7.10 | Steel Table | 50 |
| 7.11 | Safety Shield | 50 |
| CHAPTER 8. SAMPLE MATERIAL TESTED. | | 51 |
| 8.1 | Formation of the Trona Deposits | 51 |
| 8.2 | Sample Description | 52 |
| CHAPTER 9. TESTING PROCEDURES | | 54 |
| 9.1 | Testing Procedures for Pump Parameters. . | 54 |
| 9.2 | Testing Procedures for Sample Parameters. | 58 |
| 9.2.1 | Stand-Off Distance | 58 |
| 9.2.2 | Directional Property of Sample . . | 58 |
| 9.2.3 | Traverse Velocity | 59 |
| 9.2.4 | Water Jet Pressure | 60 |
| 9.2.5 | Nozzle Size | 60 |
| 9.3 | Measuring Water Jet Performance | 60 |
| 9.3.1 | Depth of Cut | 61 |
| 9.3.2 | Apparent Width | 62 |
| 9.3.3 | Volume of the Kerf | 62 |
| 9.3.4 | Rate of Removal | 63 |
| CHAPTER 10. EXPERIMENTAL RESULTS | | 64 |

| | |
|---|-----|
| 10.1 Pump Dependent Parameters | 64 |
| 10.2 Stand-Off Distance | 65 |
| 10.3 Geometry of the Sample | 66 |
| 10.4 Sample Parameter Data | 66 |
| CHAPTER 11. CONCLUSIONS AND RECOMMENDATIONS . . . | 89 |
| REFERENCES CITED | 96 |
| BIBLIOGRAPHY | 99 |
| APPENDIX | 103 |

LIST OF FIGURES

| | Page |
|---|------|
| 6.1 Manufacturer's Pump Performance Characteristics | 39 |
| 7.1 Schematic Diagram of Test Facilities | 47 |
| 9.1 Manufacturer's Pump Performance Characteristics | 56 |
| 10.1 Sample Cut at 2 Inches Per Second | 87 |
| 10.2 Sample Cut at 20 Inches Per Second | 87 |
| 10.3 Sample Cut at 12 Inches Per Second | 87 |
| 10.4 Water Jet Test Facility | 88 |
| 10.5 Water Jet at Full Pressure | 88 |

LIST OF GRAPHS

| | Page |
|---|------|
| 10.1 Volume Removed vs. Pressure at Traverse Velocity of 2 in/sec. for Various Nozzle Sizes | 72 |
| 10.2 Volume Removed vs. Pressure at Traverse Velocity of 6 in/sec. for Various Nozzle Sizes | 72 |
| 10.3 Volume Removed vs. Pressure at Traverse Velocity of 12 in/sec. for Various Nozzle Sizes | 73 |
| 10.4 Volume Removed vs. Pressure at Traverse Velocity of 20 in/sec. for Various Nozzle Sizes | 73 |
| 10.5 Kerf Width vs. Pressure at Traverse Velocity of 2 in/sec. for Various Nozzle Sizes | 75 |
| 10.6 Kerf Width vs. Pressure at Traverse Velocity of 6 in/sec. for Various Nozzle Sizes | 75 |
| 10.7 Kerf Width vs. Pressure at Traverse Velocity of 12 in/sec. for Various Nozzle Sizes | 76 |
| 10.8 Kerf Width vs. Pressure at Traverse Velocity of 20 in/sec. for Various Nozzle Sizes | 76 |
| 10.9 Depth Achieved vs. Pressure at Traverse Velocity of 2 in/sec. for Various Nozzle Sizes | 78 |
| 10.10 Depth Achieved vs. Pressure at Traverse Velocity of 6 in/sec. for Various Nozzle Sizes | 78 |
| 10.11 Depth Achieved vs. Pressure at Traverse Velocity of 12 in/sec. for Various Nozzle Sizes | 79 |

LIST OF GRAPHS, Continued

| | Page |
|--|------|
| 10.12 Depth Achieved vs. Pressure at Traverse Velocity of 20 in/sec. for Various Nozzle Sizes | 79 |
| 10.13 Cutting Rate vs. Pressure at Traverse Velocity of 2 in/sec. for Various Nozzle Sizes | 82 |
| 10.14 Cutting Rate vs. Pressure at Traverse Velocity of 6 in/sec. for Various Nozzle Sizes | 82 |
| 10.15 Cutting Rate vs. Pressure at Traverse Velocity of 12 in/sec. for Various Nozzle Sizes | 83 |
| 10.16 Cutting Rate vs. Pressure at Traverse Velocity of 20 in/sec. for Various Nozzle Sizes | 83 |
| 10.17 Specific Energy vs. Pressure at Traverse Velocity of 2 in/sec. for Various Nozzle Sizes | 84 |
| 10.18 Specific Energy vs. Pressure at Traverse Velocity of 6 in/sec. for Various Nozzle Sizes | 85 |
| 10.19 Specific Energy vs. Pressure at Traverse Velocity of 12 in/sec. for Various Nozzle Sizes | 85 |
| 10.20 Specific Energy vs. Pressure at Traverse Velocity of 20 in/sec. for Various Nozzle Sizes | 86 |
| 11.1 Traverse Velocity vs. Cutting Rate at Pressure of 15,000 psi. | 92 |
| 11.2 Traverse Velocity vs. Cutting Rate at Pressure of 23,000 psi. | 93 |

LIST OF TABLES

| | Page |
|---|------|
| 6.1 Quantity Versus Pressure for Various Nozzle Sizes | 40 |
| 6.2 Stand-Off Distance Suggested at Various Nozzle Sizes | 42 |
| 7.1 Comparison of Water Jet Pumps | 46 |
| 9.1 Identified Testing Parameters | 54 |
| 10.1 Pressures Achieved for Flow Rates Through Specific Nozzle Sizes | 64 |
| 10.2 Volume of Trona Removed for Various Nozzle Sizes | 67 |
| 10.3 Apparent Width Achieved for Various Nozzle Sizes | 68 |
| 10.4 Kerf Depth Achieved for Various Nozzle Sizes | 69 |
| 10.5 Cutting Rate Achieved for Various Nozzle Sizes | 70 |

ACKNOWLEDGMENTS

Acknowledgment is given to the Mining and Mineral Resources Research Institutes (MMRRI) fellowship fund for partial support of the research included in this thesis. The program is funded from the Department of Interiors Mineral Institutes Program, administered by the Bureau of Mines (allotment grant number: G1194108).

Haskel, Inc., provided considerable support for this research project. Its pump manufacturing division in Burbank, Calif., donated the pneumatic intensifier pump used to create the water jet tested in this thesis. Haskel's Denver area distributor provided instrumentation and equipment for the water jet testing assembly, built for the purpose of researching this thesis. A special thanks is given to Mr. John Peterson of Haskel, Inc., for his help with engineering and assembly of the equipment.

Acknowledgment is given to Tg. Soda Ash, Inc., of Green River, Wyoming, for the donation and shipment of the trona samples.

Acknowledgment is also given to Denver Machine Shop, Inc. for donated machine shop services. A special thanks is given as well to Mr. E. James White, president of Denver Machine Shop, Inc., for his help in designing parts, and for providing the use of his shop and employees for the machine work needed in this research project.

DEDICATION

This thesis is dedicated to the group of mining engineering graduate students studying water jet technology under the direction of Dr. Fun-Den Wang at the Colorado School of Mines. A special thanks is given to Dr. Wang for his dedication to helping students achieve scholastic goals by giving knowledge, guidance, and support in every way possible.

This thesis is also dedicated to my parents, Jim and Lee White, for their continuous support and friendship throughout my college education, without which I could have never attained the academic goals which I have aspired; and to my fiance Stephanie Skoog for her continuous support and devotion to my academic achievements.

INTRODUCTION

The purpose of this master's degree thesis is to present the results of a series of research experiments involving the use of a water jet as a mining tool for cutting a sodium carbonate solid called trona. Up to this point, very little knowledge has been obtained pertaining to the effectiveness with which a water jet can cut trona. Although the research found in the scope of this thesis involves simple laboratory testing, at water jet powers far lower than industry standard, the basic initial trona cutting research is presented. This research is intended to further the knowledge of cutting trona with a water jet. Knowledge of water jet principles and applications is utilized to formulate testing procedures, and the results of the test are analyzed and displayed in graphical form. Conclusions are made about the potential use of similar water jet equipment, and the potential of further research in this area, for cutting trona.

This thesis is presented in three basic parts. Chapters One through Four cover the literary research; Chapters Five through Nine describe the water jet experiment accomplished; and, Chapters 10 and 11 describe the results of the experiment and the conclusions made.

Chapter One provides a brief history of mining materials using water jets, and past research applying to this subject. An explanation of the principles involved in studying water jets, their parameters, fluid dynamics, and behavior, is presented in Chapter Two. In this chapter, types of water jets, pumping equipment, nozzle design, and mining methods utilizing water jets are described.

Chapter Three is devoted to the fluid mechanics of water jets. Some basic theories are provided, and include the work

of several investigators. In Chapter Four a literary review of research applying to rock cutting using high pressure water jets is presented.

The statement of the thesis intent is presented in Chapter Five. This chapter also covers some expectations derived from the experiment, and the limitations of the range of parameters. In Chapter Six, Seven, and Eight the parameters tested, the equipment used, and material tested are described. Chapter nine is devoted to describing the experimental test procedures.

In Chapter 10, the results of the experiment are presented graphically and described in detail. Chapter 11 is devoted to the conclusions and the recommendations.

CHAPTER 1 HISTORY

1.1 HISTORY OF MINING USING WATER

The first recorded history of utilizing the power of water as a mining tool is referred to by Pliny in his book "Natural Science," written in AD 42. This book describes the ancient Egyptian practice of running water across gold deposits in the mountains around the city of Leon in what is now northern Spain. This method of mining, known as booming, involved moving water from a reservoir down a channel to the deposit. The name booming came from the sound the water made when it first hit the sluice. Pressure was created by gravity, and then utilized to weaken the gold from the placer deposits. The high velocity which flowed from the flumes was directed across a series of trenches carved in the ore body. The water carried the ore across plant fibers laid in the bottom of a trough to trap the gold. (Summers, 1983)

In 1852, Edward D. Mathison sought a technique that would allow mining without the risk of standing close to the work area. After joining with a hydraulic engineer named Chabot, these two entrepreneurs invented the first water mining tool. Water was collected in a nail keg at the top of a 30 foot bank of sand, and then fed through a 40 foot length of Four inch diameter rawhide hose. A trumpet shaped, sheet brass nozzle was fitted to the end of the hose inside a wooden jacket. The first test took place at the American Hill Mine near Nevada City, Nevada. The hose was converted to canvas and the nozzle made of solid brass by the time the experiment had its public demonstration in June 1853. This first mining water jet was called a monitor.

Between 1871 and 1880, 425 companies utilized the crude monitors to produce thousands of tons of gold ore, worth millions of dollars at that time. A typical monitor could mine as much as 10 cubic yards of ore per day. These monitors were eventually equipped with crude pumps, replacing the original gravity formed pressure head. (Frank, Fogelson, and Chester, 1972)

In 1867, hydraulic monitors were imported to Russia for mining gold in the deposits surrounding Lake Baykal. By 1890, the Russians had successfully reduced their mining operating costs by 60 percent. The technique was also utilized to mine peat, and, by 1914, 30 percent of all peat mined worldwide was mined using water monitors.

The first underground trials of a water jet mining system took place in the shaft of a coal mine in the Donet Basin (Donbase) in 1915. V.S. Muchnik was the first researcher to write a thesis on water jet technology for mining coal in 1935. By 1939 the first operating underground hydraulic mine was opened at a gold operation near Lake Baykal, Russia. (Summers, 1983)

After World War II, much debris required moving for reconstruction of Europe. Hydraulic mining accounted for 60 to 70 percent of this, moving some 100 million cubic yards of material between 1947 and 1950. (Frank, Fogelson, and Chester, 1972)

Coal was first mined commercially by this method starting in 1952 at the Tyrganskies - Uklong mine in the Kuznetsk Basin of Russia. Six hundred psi (pounds per square inch) of water was used to wash away preblasted coal at the rate of 600 tons per shift -- more than twice the conventional levels of production in the area at that time. A second mine was converted in 1953, again using water jets to wash away preblasted coal. (Summers, 1983)

By 1957, with the development of higher pressure pumps, the monitor pressure was accelerated to a sufficient level to avoid preblasting of coal. The practice of using water to wash preblasted coal was never used after that time.

1.2 DESCRIPTION OF EARLY MONITORS

Monitors utilized for mining and earth-moving practices were hand operated, and were equipped with large wheels. Deflectors were employed to help the operators with monitor mobility. These machines had operating pressures under 1000 psi, and could mine about 130 cubic yards per hour. Initially, monitors were used in open-face mining operations. A miner could stand back a sufficient distance from the face for safety, while sweeping the high pressure jet across the face. Ore would fall to the ground, where it could be either washed into a pile or collected directly under the working face. (PEELE, 1939)

1.3 GROWTH OF MONITOR TECHNOLOGY UNDERGROUND

The achievement of improved technology in the development of hydraulic monitors created opportunities for experimentation with new mining methods utilizing the equipment. An attempt was made in the Soviet Union to mine vertical seams of coal by first boring a hole down through a seam to an adjacent sublevel. A water jet was then attached to the drill head from the lower level, and was slowly raised while the water jet was rotated. The coal would fall to the underlying entry for transport. Americans investigated this new method, and employed it with success at the American Gilsonite Operation in the Green River Basin, Utah, in 1957. In this application, two car-mounted monitors were used to

mine about 1,000 tons of Gilsonite per shift. Twelve feet high benches were driven at a 2.5 degree grade. A flume at one side acted as the transport system between two shafts at 1,000 foot centers. (Frank and Fogelson, 1972)

In 1961, a water jet was mounted on the bottom of a raise boring drill. The drill was first used to drive a six inch hole for 600 feet downward to a collection drift, and then, with the jet head operating, it was slowly retracted back up the hole at one round per minute while material fell into the borehole. This drill was raised by hand and average production achieved was about 600 tons per eight hour shift.

The success of this mining method led to trials of a similar method in coal seams in Canada. Unfortunately, the seam was too shallow to disperse the coal cuttings into a collection flume and was therefore abandoned.

Following World War II, investigators from the United Kingdom visited the monitor sites in Russia to find an improved method of mining. These investigators experimented with water monitor mining at the Travis Drift Mine in Wales. A series of tests were carried out to find improved methods of water jet cutting for mining British coal seams. The investigators concluded that the coal seams in the United Kingdom were not steep enough for success. However, their experimentation helped in the area of improving the distance with which the jet stream was an effective cutting tool.

Particular interest was next focused on straightening the flow into the nozzle from the supply line. It was found that if the flow was very turbulent, with a spinning action the length of the supply line directly behind the nozzle, that the nozzle will have a more coherent jet.

Investigators in Japan used extremely long nozzles, similar to the ones used in gold mining in California in the past. These were found to steady the flow after the jet

reached the swivels, and before it reached the nozzles. The British achieved similar results by inserting flow straighteners in shorter nozzles. (Summers, 1983)

Leach and Walker have perhaps done the most significant work in nozzle design for optimum jet performance. Their studies involved nozzle shape and found that a 13 degree nozzle, from centerline conically outward, would produce a very coherent jet. (Leach and Walker, 1966)

At the same time as these studies were being conducted in England, the U.S. Bureau of Mines began research in this technology. Tests were initially carried out using hand-held monitors. A series of tests were conducted in anthracite coal using the first remotely-controlled monitor operated from a control center, mounted on the machine. The monitor head was able to move both vertically and horizontally across the coal face. Due to the necessity of having men handle the equipment, only low production rates were realized. For the next 10 years, little research was carried out in the United States or England in hydraulic mining.

1.4 WATER JET ASSISTED MECHANICAL MINING

Investigation of water jet assisted mechanical mining was the focus of water jet study from the mid 1970s to the early 1980s. The technology has been studied for applications in percussive drilling, oil well drilling, tunnel boring, and continuous mining. These studies indicate that rock can be cut at a lower mechanical force, by assisting a mechanical tool with a water jet, then the forces associated with cutting with mechanical tools only. Water jets lead the mechanical tool to create new free surfaces allowing the rock to break toward them, providing a greater entry for the mechanical tool to achieve a greater penetration rate. (Wang, 1976)

In mining applications, three types of water jet assisted mechanical excavation have been recognized. Full face equipment such as a tunnel boring machine (TBM) using a disc cutter and assisted by water jet, partial face cutting with a boom or drum cutter using water jets to assist individual tool cutting, and peripheral slotting with kerfing tools. (Wang, 1976)

When a water jet assists the mechanical tool, increased penetration of the tool is realized with reduction of tool forces. As the mechanical tool penetrates the rock and forms a crushed zone, with fractures extending outward, the water jet penetrates the crushed zone and hydrofractures it. The jet aids the fracturing process by extending fractures and removing crushed material from the immediate region, thus creating a free face for the mechanical tool. (Wang, 1984)

Assisting mechanical methods with water jets has the advantage of reducing the cutting forces required for higher strength rocks, reducing machine vibration and dust levels, and improving machine bit wear. Also, harder rocks can be cut with water jet assisted mechanical mining.

1.5 MINING METHODS UTILIZING HYDRAULIC MINING

Many hydraulic mining methods borrow technology from other methods of mining. Initially, the water jet monitor was used in placer and other surface mining methods. It eventually became a useful tool for mining underground.

Success in surface mining depends on certain conditions which must be met. Availability of clean water, a moderately warm climate and adequate space must all exist. The terrain must have some slope for gravity fluming of material and tailings disposal. Perhaps the most important condition is

that there are minimal regulations controlling fine disposal and reclamation. It is this last stringent condition which eventually closed all hydromining operations in the gold rush days of California.

Hydraulic mining has been experimented with and practiced in many soft material mines underground, the most prominent being coal seams with some degree of dip. Most methods of underground hydraulic mining are similar to methods of conventional mining practiced in the past. For example, in coal, a water jet can be mounted in place of a conventional cutting head on a continuous mining machine. Water jets can also be stationary, as in the early Russian research, or mounted on mobile units. With a water jet as a tool, mining has been accomplished using room and pillar, cross pitch, longwall, sublevel mining, and longhole retreat methods.

Room and pillar mining can be used to create rooms in a seam, or to remove old pillars in existing workings. A continuous water jet miner equipped with a loader could be utilized for this method in softer rock types.

Longhole hydromining applies very readily to water jets. A long hole is drilled from an upper level to a lower level in a steep coal seam, then a jet is placed on the cutter head and retracted slowly, with a rotating water jet cutting to a desired radius. Coal then falls to the lower level for transport. Caving methods and methods of sublevel stoping can also be accomplished in a similar fashion.

Although many methods have been tested and utilized in hydraulic mining, there has been little interest in these methods of hydromining. It should be stressed that many of these methods involved lower pressures and higher flows, due to a lack of technology in the pump and water jet fields. Greater interest in using water jets combined with mechanical cutting heads in hydraulic mining experimentation was seen in

the 1970s. The U.S. Bureau of Mines did significant testing using high-pressure nozzles mounted on the cutters of road headers and TBMs. Results of these investigations showed much promise. However, they did not achieve commercial success due to the water filtration methods and low production lives of the high-pressure equipment used that made these methods economically infeasible. It is believed that with improved water jet machinery, at higher production lives and higher pressures, as well as with better filtering methods, a water jet can be utilized to economically cut coal and rock.

CHAPTER 2

HIGH PRESSURE PUMPS AND TYPES OF JETS

Water jets can be used in a variety of applications, and many types of jets are now commercially available. The cleaning industry has utilized continuous and abrasive jets for the past 20 years. These jets are generally lower in pressure and higher in volume than other jets used in industry. Cutting jets are used extensively in the industrial sector. For example, most interior portions of automobiles, such as dash boards and seat covers, are commonly cut with water jets. Industry also uses water jets to cut garbage bags, diapers, cardboard boxes and many other products. The mining industry was the first to utilize high pressure water jets outside of the fire-fighting industry.

2.1 HIGH PRESSURE PUMPS

A jet is formed when water, or other fluid, is forced through a nozzle at high pressure. This pressure can be created by gravity, as seen in the history of hydraulic mining, or with a pressure-forming pump. The most common method of creating high pressure is with a high pressure pump. Many types of pumps have been created, tested, and utilized and each has unique benefits.

Centrifugal pumps are particularly noted for their ability to pump very high volumes with relatively low pressures. These were the first pumps used with water jets because technology permitted the seals for these pumps to be readily available at this time.

Plunger pumps are direct-driven, crank-style, positive-displacement units. These pumps have between three and five

pistons, and are called triplex or quintex pumps, respectively. These pumps have the ability to pump high volumes of 10 to 500 gallons per minute (gpm) at pressures limited to the range of 5,000 to 30,000 pounds per square inch (psi). These pumps have been used extensively in the cleaning industry, where higher volumes of water at relatively high pressures are needed. They also show promise for the coal and soft rock mining industry, utilizing the higher flows as the cutting mechanism. (Summers, 1974)

An intensifier pump is a duplex plunger pump, usually driven either hydraulically or pneumatically. In most applications, the driving medium is applied to a large piston, causing it to reciprocate back and forth. The large piston is attached to two smaller plungers which come in contact with the high pressure water. The high-pressure water seal is stationary, and the plunger displaces the water in the high-pressure cylinder cavity. Check valves on the inlet and outlet of the high pressure cylinder control the flow of water to and from the high pressure section of the intensifier. The reversal of the piston motion is controlled by limit switches which shift a directional valve, changing the flow of the driving medium into the low-pressure medium cylinder. (Labus, 1991)

Hydraulic intensifier pumps utilize hydraulic oil as the driving medium. These pumps can achieve pressure ranges from 30,000 to 100,000 psi at a flow rate of one to seven gpm. Separate intensifiers can be set parallel with each other to attain flow rates in excess of 30 gpm at similar pressures. These pumps can produce water jets which cut hard rocks, steel, and a variety of other composite materials. (Labus, 1991)

Air driven intensifier pumps are identical to linear, hydraulic intensifier pumps, except that the driving medium is

air. These pumps can produce working pressures over 20,000 psi and flow rates up to one gpm. The principal advantage to this pump over a hydraulically-driven pump is capital cost. The pump can also be used in the field with a portable compressor where no electric power is available. (Labus, 1991)

2.2 TYPES OF JETS

With existing pumps, disturbing the continuity of the jet can cause different cutting actions. In the simplest form, the jet is utilized as a continuous, steady jet. Basic jet types include:

1. Continuous, "water only", and abrasive;
2. Pulsed, culmination, pressure extrusive, and percussive; and,
3. Cavitating

2.2.1 CONTINUOUS JETS

The continuous jet is the most widely used jet in industrial applications. When water is used as the fluid medium, a water jet is formed. Theories have been devised to demonstrate limited modeling ability in jet performance when cutting different materials. However, the most common practice is to test the subject to obtain reliable data for systems design. This testing can provide a direct correlation between the jet parameters and material behavior. Continuous jets are best suited for cutting softer materials.

If abrasive material is introduced to the cutting action of the jet, an abrasive jet is formed. Abrasives are introduced by use of a mixing chamber, or mixing tube, out of which the water/abrasive jet is then applied directly to the material. Water is used to accelerate the abrasive particles

to a terminal velocity before they impact the target surface. Some experimentation has taken place to inject the abrasive either before the pump, or before the nozzle. Abrasive jets are used extensively in industrial applications which require higher cutting forces than continuous jets can produce. Promise exists in the mining industry to use the water jet for peripheral cutting on the boundary of a drift or bore hole. (Labus, 1991)

2.2.2 PULSED JETS

Pulsed jets are characterized by their L/D ratios (slug length to diameter), method of generation, and energy content. The type of failure produced by pulsed jets is semi-controlled fracture propagation which results in the removal of large, irregular pieces of material from the target surface. These jets demonstrate higher volumetric removals, utilizing lower energy, and thus tend to have lower specific energies. They have little dimensional control, but, this is not necessarily an important condition for mining applications. Culmination jets create pulses with a high energy content, short pulse duration, and small fluid content per pulse. They can create large-scale, fracture-based failure. Culmination jets have a maximum velocity which is dependent on nozzle area ratios, rather than on nozzle diameters, which are related to nozzle length and water slug length. (Labus, 1991)

A pressure extrusive jet also creates large-scale, fracture-based failure. It does this by creating a sustained jet velocity with respect to time and pulse generation. Its maximum velocity is dependent on the area of the nozzle, and is thus related to nozzle diameter. There is generally a large fluid volume in each pulse, hence the name "water cannon" which has been given to pressure extrusive jets. This type of

jet has the power to blow a one inch diameter hole in a 1/8 inch steel plate with one slug of water at a 40 foot distance. There is much promise in this type of jet for rock breaking and comminution. Research is currently being done in this area. (Wang, personal communication)

Pulse jets are predominately in the development stage at this time. However, these jets show the greatest potential for mining and construction.

2.2.3 CAVITATING JETS

A cavitating jet is a continuous jet in which cavitation is purposely induced. In the past, cavitation in the jet was strongly discouraged, as improper cavitation could cause great damage to the nozzle and other parts of the water jet. In this jet, cavitation bubbles composed of gaseous water or fluid medium, rather than air, are created and carried downstream, where they ideally collapse at the target surface. These collapsing bubbles induce large surface stresses and micro jets. Cavitating jets create a wider kerf than continuous jets and have the distinct advantage of having system hardware that can be greatly simplified, in terms of operating pressures, to create the same damage. One of the greatest current setbacks is the control of the system components, such as nozzles, which, if not engineered properly, can have very short lives. Research is currently being done on cavitating jets. (Labus, 1991)

CHAPTER 3
FLUID DYNAMICS OF WATER JETS

Fluid dynamics of water jets is a very broad subject that will require considerable research and investigation in the future to obtain a full understanding of the topic. What is known to be true to date is that the fluid dynamics portion of a jet -- from the time water reaches the filters, goes through the filters to a pump system, and through the pump system to the nozzle orifice. These fluid dynamics properties have been investigated by numerous researchers and many books have been written to explain the fluid dynamics of a pumping system. Perhaps the most influential authority of classical fluid dynamics is Bernoulli. What is lacking in fluid dynamics research of water jets is what happens to the jet stream after it passes through the nozzle orifice until the time its power is negligible.

The most complicating factor of this research is that when the jet enters the atmosphere, it picks up ionic portions of the atmospheric medium and turns into a three- phase flow. In the first phase, pure water makes up the critical stream of the jet. In the second phase, air mixes with the jet upon the phase contact between the immersing jet and the atmosphere. The third is a gaseous phase of water created by the high pressure of the stream. For this three-phase jet, no exact mathematical approach completely explains the fluid dynamic phenomenon.

What is known is that there is a definite relationship between pump pressure, volume flow rate, and nozzle shape and size. The density, viscosity, and surface tension of the jet's fluid medium also effect the observed behavior of a jet. When water is used as the fluid medium, these parameters are

a certainty. However, contrary to classical fluid mechanics principles, water is compressible at the high pressures created in a water jet. This compressibility changes, from jet to jet, depending on the pressure. For this reason, density, viscosity and surface tension can never be truly known without copious testing of each individual jet. This was not a significant issue at the pressures used for this work.

Some applications in the water jet industry introduce a long-stream polymer to the fluid of the jet, thereby changing the above parameters to achieve better results in jet performance. One brand name given to this polymer is "Super Water," and has been substituted for the name "long chain polymer addition" in the industry. The performance parameters in this case are, at best, only truly known by testing individual jets.

To complicate matters even more, each type of jet -- continuous, pulsing, or cavitating -- displays different results in jet parameters from one type to another.

Many researchers have attempted to explain the simplest form of jet, the continuous jet, by "rules of thumb" and/or models created for particular applications. Due to diverse ranges of particular test parameters and assumptions, conflicts have occurred in the final results of every case.

What is observed in all attempts are certain inherent fluid dynamics principles. In each approach studied, there is an observed relationship between pressure and volume, and all approaches provide a factor added in that accounts for surface tension and other losses occurring at the nozzle. The only way to account for discrepancy in these methods is to assume that every jet tested to formulate models, compressibility factors, or special variables to account for jet behavior, is different than the rest. And, if this is the case, the only

way to know the variable to use for a particular jet is to test it individually.

All methods start with Bernoulli's equation -- between any two points of flow, and with an equation for continuity between any two points of flow.

Bernoulli's equation, neglecting the elevation terms, which are negligible assuming the water goes into the pump at the same elevation as it comes out, states:

$$\frac{P_1}{\rho_1} + \frac{(V_1)^2}{2} = \frac{P_2}{\rho_2} + \frac{(V_2)^2}{2} \quad (3.1)$$

Where:

P = Static Pump Pressure
 V = Average Fluid Velocity
 Rho = Average Fluid Density

The continuity equation states:

$$\rho_1 V_1 A_1 = \rho_2 V_2 A_2 \quad (3.2)$$

Where:

Rho = Average Fluid Density
 V = Average Fluid Velocity
 A = Area

Utilizing these two relationships of flow, and neglecting the compressibility of water, surface tension, and all other properties exerted by the fluid medium, the exit velocity of

a jet can in theory be expressed:

$$(V_2)^2 = (V_1)^2 + 2 (P_1 - P_2) \rho \quad (3.3)$$

And, if the pressure is assumed to be equivalent on both sides of the nozzle, and

$$A = \Pi \frac{d^2}{4} \quad (3.4)$$

Then, the continuity equation can be expressed:

$$V_1 (d_1)^2 = V_2 (d_2)^2 \quad (3.5)$$

Substituting this into Bernoulli's Equation:

$$(V_2)^2 = (V_1)^2 \left(\frac{d_2}{d_1} \right)^4 + \frac{2 (P_1 - P_2)}{\rho} \quad (3.6)$$

Or:

$$V_2 = \sqrt{\frac{2 (P_1 - P_2)}{\rho \left(1 - \left(\frac{d_2}{d_1}\right)^4\right)}} \quad (3.7)$$

Taking into account all of the above assumptions, and if V_2 is the exit jet velocity, then the above relationship provides an expression with which to begin for finding jet performance relationships.

The flow rate can also be found since:

$$Q = VA \quad (3.8)$$

Where:

Q = Quantity Flowing
 V = Velocity of Flow
 A = Area of Nozzle Opening

These equations of flow assume a discharge coefficient for a Leach and Walker type nozzle, which is in the order of 0.7. (Labus, 1991)

T. Labus gives some equations to get close to actual values using observed "rule of thumb" factors and unit conversion factors:

Flow Rate:

$$Q = 29.826 \underline{c} d^2 \sqrt{\Delta P}, \quad \text{gpm} \quad (3.9)$$

Jet Velocity:

$$V = 12.184 \sqrt{\Delta P}, \quad \text{ft/sec} \quad (3.10)$$

Where:

$$\Delta P = \text{Pressure drop} \quad (3.11)$$

Jet Thrust:

$$T = 0.05266 Q \sqrt{\Delta P}, \quad \text{lb.} \quad (3.12)$$

Power:

$$P = Q \frac{(\Delta P)}{1714}, \quad \text{hp} \quad (3.13)$$

T. Labus' approach to jet fluid dynamics is the most straightforward in terms of classical fluid dynamics. However, the simplest approach is that of J. Olsen in his study of jets for Flow Systems, Inc.

Suggestion is made that the Bernoulli equation can represent the jet velocity regardless of the upstream pipe diameter. This velocity is:

$$V = \sqrt{\frac{2P}{\rho}} \quad (3.14)$$

Where:

V = Jet Velocity
P = Pump Working Pressure
Rho = Fluid Density Factor

In this equation, the density term is actually a factor which takes into account the compressibility of water of 12 percent value. The value used by Olsen for this factor is the average density between compressed water and water at atmospheric pressure. This equation is also dependent only on pressure, and not on any geometric feature of the nozzle.

Geometry is accounted for in the discharge coefficient factor, as is the case with Labus' approach.

Given:

$$Q = VA \quad (3.15)$$

And:

$$A = \frac{\Pi d^2}{4} \quad (3.16)$$

Where:

d = Nozzle Diameter

Substituting into Equation 14, a relationship for quantity of flow can be expressed as:

$$Q = c \frac{\Pi d^2}{4} \sqrt{\frac{2P}{\rho}} \quad (3.17)$$

The equation for nozzle power in this method is again:

$$W = PQ \quad (3.18)$$

or

$$W = c \frac{\Pi d^2}{4} \sqrt{\frac{2}{\rho}} P^{3/2} \quad (3.19)$$

when expressed in Equation 17. for quantity.

This relationship specifies that if two parameters of the jet are known, such as pressure and nozzle diameter, the remaining unknowns can be calculated. (Olsen)

The last two examples of calculating the relationships of

jet performance characteristics display what is known to be true for given situations. Many researchers have used testing methods for determining fluid dynamics of a particular water jet. In this approach, a previously calculated manufacturer's pump characteristic curve for quantity versus pressure can be used. If one or more variables are tested, other variables can be found using previous pump data.

CHAPTER 4
WATER JET ROCK CUTTING

Research has been accomplished on the physics of water jet cutting through many composite materials, including rock. One of the first investigations on the theory of a water jet's mechanism of rock destruction is "Examination of High Pressure Water Jets For Use In Rock Tunnel Excavation." The directors of the project working under a Civil Defense Research Project, were W.C. McClain and G.A. Cristy. Their first work was completed in 1969 and formally written by 1970. Primary rocks investigated were sandstone, limestone and granite. This work is of particular interest in understanding the mechanism of rock destruction.

McClain and Cristy suggest that the rate of advance of a cutting water jet in rock is related to the specific energy of the jet and the rate at which energy can be applied to the rock. When a piece of rock is broken, energy is consumed in creating a new surface area. A certain maximum force, or energy, is required to overcome the strength or cohesion of the rock before the disintegration process begins. Once these threshold levels of force or energy have been exceeded, the amount of energy required to remove a unit volume of rock remains nearly constant for a given rock (Chermensky). This parameter -- the energy required to remove a unit volume of rock -- is called the "specific energy," and is related to linear rate of advance as:

$$R = \frac{P}{AE} \quad (4.1)$$

Where:

R = Linear Rate of Advance
P = Power Transmitted to the Rock
A = Cross Sectional Area of Tunnel or Hole
E = Specific Energy

The specific energy is the factor determining how fast a tunnel, or hole, can be cut using water jets for different types of rock. (Chermensky)

Another prominent series of studies was performed by S.C. Crow, whose research was devoted to the theory of hydraulic rock cutting. His model incorporates fluid dynamics principles with rock properties for effective destruction of rocks.

Crow has demonstrated the method of destruction for a specific water jet utilizing a mathematical model, and has successfully compared his empirical approach to experimental values in "The Theory of Hydraulic Rock Cutting." This empirical approach is explained, and later edited to include material porosity (Crow, 1974). In this theory, a mathematical model is created and used to explain cutting of specific rocks with water jets.

The rock is assumed to translate at a traverse speed across a continuous jet for the purpose of determining the depth of the resulting slot as a function of feed rate, the diameter of the jet, total jet pressure, and the relevant properties of the rock.

In this theory, the jet exerts traction against a cutting surface at the leading edge of the slot, and the traction induces continuous fracture. Cavitation tends to sheath the cutting surface in vapor, but curvature of the jet stream causes high surface pressure which closes the cavity bubbles and exposes the grains to direct impact from the water. The

surface pressure would suffice to keep the grains in place, but permeability allows the water to penetrate beneath the cutting surface and relieve the pressure across the grains (Crow, 1974).

Permeability gives rise to an intrinsic speed for rock cutting which is related to the permeability, shear strength and internal friction of the rock, and the rock grain size. It is found that the kerf depth, or depth of the cut, decreases as the velocity comes equivalent to the intrinsic speed. (Crow, 1974)

These two approaches to water jet research were preceded by the work of several groups studying a variety of applications of water jet technology.

Early research in the area of hydraulic rock cutting theory was performed by Farmer and Attewell, who tested continuous water jets against fixed targets. As a qualitative model of penetration, it was assumed that the jet impacted the free surface of the rock as a "train of solid projectiles," and deformed the rock plastically by momentum transfer. An empirical formula for the depth of penetration was prepared using experimental data. The formula was not consistent, however, with the momentum transfer argument. (Farmer and Attewell)

Leach and Walker were the next investigators to study water jets cutting fixed targets. The main concern of this research was the effect of nozzle shape on the coherence of the jet. It was discovered that penetration could not be achieved if the total pressure of the jet stream was below a critical pressure, dependent on rock type. The depth of penetration appeared to be proportional to the difference between the pump ambient pressure and the critical pressure. This difference was called the constant of proportionality, and, again, was dependent on rock type. It was also found

that a high constant of proportionality did not imply a low critical pressure. It was concluded that fracture and final depth of penetration are controlled by different mechanisms (Crow).

The next group of researchers to follow was Brook and Summers. They studied penetration into static targets as a function of stand off distance -- the distance between the nozzle orifice and the target. Also included were driving pressure and duration of the jet stream. The penetration depth was found to be proportional to the driving pressure and duration of the jet stream. Driving pressure rose rapidly in the first few milliseconds of jet impingement, then much more gradually with increased time. Because the target material was sandstone, a critical pressure could not be observed. This could be due to the materials porosity or strength (Brook and Summers).

Powell and Simpson attempted to calculate the critical pressure on the basis of elastic theory and fracture ability. Experimental results were found to be better in terms of rock cutting than those found by Brook and Summers. Their conclusion was, "The rock cutting action of a water jet cannot be explained entirely in terms of mechanical fracture due to the stress field induced internally in the rock by the impact of the jet". (Crow)

Crow was the next researcher to continue work in this field. He attempted to explain the mechanics of hydraulic rock cutting by going beyond the fracture criterion, and on to the relationship between the fluid mechanics of the jet stream and the solid mechanics of the rock, as was the case in previous papers. Crow introduced a mathematical model involving many complex variables from both the fluid mechanics and fracture criterion. Variables included cavitation, brittle fracture permeability, porosity, among others. This

model is currently the most complete explanation of hydraulic rock cutting, and presumably works with moderate success (Crow, 1974).

Although Crow's model is successful, many researchers have not utilized it for practical rock cutting applications. This is due to the complex nature of variables which are very difficult to measure. In many cases, a full-scale rock mechanics testing procedure is needed. (Wang, personal communication).

The other option offered to researchers for finding the hydraulic cutting capability of a jet on a particular rock type is to test individual jet parameters on the target surface. This is much simpler than the modeling method Crow used, and more accurate results can be expected. This justifies the experimental approach taken in this thesis. (Wang, personal communication).

CHAPTER 5

STATEMENT OF THESIS INTENT

5.1 OBJECTIVE OF THESIS

The objective of this thesis is to determine the ability of using a water jet to cut trona, a sodium carbonate material commonly mined in southwest Wyoming. Water jets have successfully cut a number of soft rock materials, such as coal, and in some cases, harder rock materials such as granite or marble. Trona can be cut using continuous mining tools, as it is relatively soft and brittle, but harder than coal. Experimentation has been accomplished in drilling trona with water jets with a mild degree of success, although no practical application has occurred.

In determining the ability of cutting trona with water jets, several factors are considered. The key parameters of a water jet are identified and tested, and the relationship of these parameters with certain material properties of the trona are addressed in the scope of the experiment.

With these parameters identified, they are tested and evaluated for the ability of using a water jet as a trona cutting tool.

It is anticipated that some of the basic scientific information, applying to cutting trona with water jets, will be found, warranting future testing in this area. With the research accomplished in this thesis, it is hoped that future research can lead to trona mining with water jets being used as the principle mining tools.

5.2 APPROACH TO THESIS OBJECTIVE

The approach taken to achieve the objective of the thesis was to identify and accomplish three goals pertaining to the water jet testing program. The first goal was to assemble the water jet out of existing equipment, and to understand its limitations and capabilities. The second goal was to identify the parameters pertaining to the water jets performance, and to apply this knowledge in planning a reasonable testing sequence. The third goal was to identify the relationship of the parameters to minimize testing and maximize results.

5.2.1 EQUIPMENT SET UP

Perhaps the most important, and rigorous, of the three goals identified was the actual assembly of the water jet equipment. The equipment set-up is explained in detail in Chapter Seven. After the equipment was assembled and tested, it was calibrated and studied. Next, parameters critical to the experiment were identified.

Parameters which are pertinent to the equipment are the output water pressure and volume, the input energy, and the variable equipment, considering factors such as nozzle sizes.

Gauges and other means of parameter measurement were needed to define the optimal cutting parameters. Pressure of the compressed air, which is the intensifier pump's driving energy, was measured directly in-line before entering the pump. Output water volume was measured using a low-pressure flow meter on the inlet side of the pump. Output water pressure was measured by utilizing the pump characteristic curve (shown in subsequent chapters) and other measured input data including the use of Bernoulli's equation for liquid states and a continuity equation.

A pre-charging pump was utilized in-line with the water jet pump and water filters assembled prior to the pump.

The samples were traversed across the water jet on a variable speed, rodless cylinder. This cylinder was measured directly for velocity with a digital stop watch.

5.2.2 PARAMETERS APPLYING TO RESEARCH

The parameters that are addressed include the basic parameters of water jet study. Water pressure created by the jet, combined with the jet's output volume, constitute the cutting force of the jet. These two variables are related to each other. A higher pressure can be created by restricting the flow of the water jet through yet another parameter, the nozzle size. The water pressure can also be varied by increasing the pressure of the compressed air driving the water jet pump. This was accomplished by reducing the flow of the air in a regulator. By applying the relationships of the above parameters, the water jet can be controlled and varied for different cutting results.

Parameters which are not directly related to the water jet, but are very important to the cutting ability in the trona, include the distance of the jet from the target, the velocity of the water jet passing across the target, and the direction on the trona sample in which to test. The distance from the water jet nozzle to the target is commonly referred to as the stand-off distance. This parameter is optimal when the shortest distance is used. However, there is a minimum distance from the jet nozzle to the sample which does not effect the cutting ability of the jet. The traverse velocity is the speed with which the jet nozzle passes across the sample. This parameter is very important in determining the speed with which an amount of trona can be cut. This parameter was simulated by passing the sample across the stationary jet. The sample of trona is inconsistent in its

crystallinity, and has a definite bedding plane. Therefore, certain sample parameters exist. The sample can be traversed across the jet, perpendicular or parallel to its natural bedding plane, or in a third direction perpendicular to the strike of the bedding plane.

All of the identified parameters are addressed in the scope of the research to find the trona cutting effectiveness of the water jet.

5.3 SCOPE OF THE RESEARCH

The identified parameters of the water jet are tested in a manner that will yields the best cutting effectiveness of the jet. This was accomplished in a variety of ways, and it was the intent of the research program to find the most efficient sequence of testing to do so. Included are the equipment assembly; calibration; methodology of measurement of equipment parameters; the sample preparation, which includes optimal sizing and surface requirements; and, the sequencing of parameter measurement.

The sample preparation is included in detail in Chapter Eight. Each sample was cut to a size convenient to being traversed on the traverse mechanism, and in a way that utilizes the bedding plane to its best advantage. Because of this, the samples directional cutting parameters were tested first, so that sample preparation could be accomplished accordingly. The jet was only tested for single passes on the trona for the scope of this thesis.

The next parameter addressed is the stand-off distance. A minimal stand-off distance was studied in the literature, and is calculated in Chapter Six. This parameter was tested to find a maximum distance at which the sample can be placed and not effect the cutting ability of the water jet.

After the previous testing, two groups of parameters were addressed for the testing sequence. These were the water jet equipment parameter relationships and the sample traversing parameters.

Next, the relationship of the nozzle size of the jet to the pressure and volume output of the water jet was found for different input driving air pressures delivered to the pump. To optimize these parameters for the cutting ability of the trona, the pump was investigated. This sequence of testing involved finding pressures and volumes delivered by the water jet at respective input air pressures delivered for each respective nozzle size. Since all nozzle sizes have unique pressure ranges within the power of the pump, each nozzle was tested for a unique set of pressures. Nozzle sizes were identified for optimal water jet power to optimize the cutting action of the jet. The selection of these nozzle sizes, and the relationship of the test program, are covered in detail in Chapter Six. The parameters involving the traverse velocity, and method of finding them are also clearly defined in Chapter Six.

The testing sequence, after all of the parameters were defined, involved testing individual sets of parameters to cover all parameter scenarios. A total of four nozzle sizes were tested at four traverse velocities for three separate water pressures. After this, two nozzle sizes were tested for a fourth pressure. They are identified in Chapter Six, where specific parameter values are utilized. These include a full range of pump pressures and traverse velocities available from the rodless cylinder used, and the range of nozzle sizes which incorporate the best cutting nozzle size within the range. In the results of this thesis, it is shown that all parameters tested incorporate the effectiveness of using a water jet to cut trona.

CHAPTER 6

WATER JET PARAMETERS

In an attempt to test a water jet for cutting any material, certain parameters must be tested and optimized to see their full potential. These parameters are: the pressure to volume ratio, which is related to jet stream velocity and nozzle size; the optimal stand-off distance, which is controlled by the size of the central core region of the jet; the traverse velocity of the jet, which is simulated by passing a sample at constant velocity across a steady jet stream; and, the effect of the material's direction of feed, which is tested by cutting with and against the bedding plane. Other tests which are held constant, due to restrictions in equipment, are the effect of nozzle shape and design, and the effect of angle of inclusion of the jet.

6.1 PRESSURE TO VOLUME RATIO

The pump tested allows a range of peak volumes to be delivered at respective pressures. These tests are predetermined, and described on the manufacturer's pump performance curve chart, however, pressures may also be calculated using fluid dynamics principles. In general, a higher water volume can be pumped at a higher water pressure, governed by the driving pneumatic pressure and volume delivered by an air compressor. It is very possible that pumping a higher water volume at a lower water pressure will allow for greater breakability of the trona. This will be the case if there is an overabundance of driving air. The water jet volume and pressure can be regulated by either changing the driving air pressure which constricts the air flow, or by

changing the nozzle size which restricts the water flow and increases the water pressure with smaller sizes.

6.2 NOZZLE SIZE

Assuming a maintained, constant input driving air pressure, maximum performance can be achieved in cutting when using the pump by varying the nozzle sizes. The pump will, at best, deliver volumes at pressures governed by the pump characteristic curve. Using Olsen's "rule of thumb" equation for volume flow rate described in Chapter Three, and including a discharge coefficient of his recommended 0.7, an envelope of nozzle sizes which will allow volumes to flow at pressures similar to those seen in the pump characteristic curve can be identified. Because of questions as to the reliability of the assumption that this equation and its discharge coefficient are correct, the nozzle sizes in the envelope must be tested for performance. As previously stated, assuming a maintained, constant input driving air pressure, a maximum performance can be achieved for the pump by varying nozzle sizes. The idea here is to match volumetric fluid dynamics principles for high pressure flow through the nozzles -- with the indicated performance curve points for input driving air pressure -- to maximize output water jet pressure at peak volumetric pumping performances. As a predictive start, the fluid dynamics principles of Olsen, briefly described earlier, will be used to find the range of nozzle sizes to test. Recalling the compressibility factor for water at high pressure, and Bernoulli's equation for incompressible flow, Olsen's equation relating pressure to volume is:

Where:

$$V = \sqrt{\frac{2P}{\rho}} \quad (6.1)$$

V = Velocity of Flow
 P = Pressure
 Rho = Density of Fluid

Recalling that Conn described the velocity of the stream in terms of out put pressure only, and not for this "rule of thumb" equation on any geometric feature of the nozzle, and taking into account the classical fluid equation for flow:

$$Q = VA \quad (6.2)$$

Where:

Q = Flow Rate of the Stream
 A = Area of the Stream
 V = Velocity of the Flow

Where the area of the stream can be related to the diameter of the nozzle, a relationship can be found between the nozzle diameter and the flow rate of the water jet. A term that needs to be included in the above equation for quantity is the discharge coefficient, which is related to nozzle geometry. This is described as the compressibility factor, and is on the order of 0.7 for the standard nozzles used in this experiment.

Olsen describes the flow rate through the nozzle as:

$$Q = c \frac{\pi d^2}{4} \sqrt{\frac{2P}{\rho}} \quad (6.3)$$

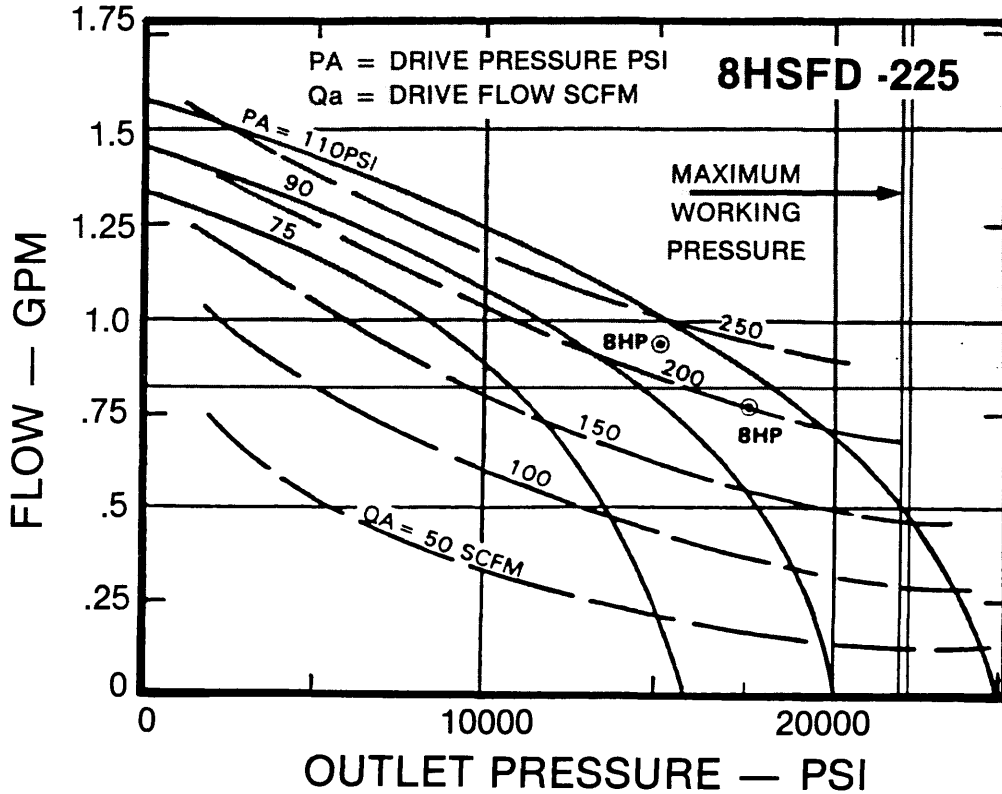
Where:

c = Discharge Coefficient
d = Nozzle Diameter
Q = Volume Flow Rate

Assuming that Olsen's equation is correct, a relationship can be found using calculations for water pressure and volume only, given the nozzle diameter. When these values are compared to the manufacturer's pump performance characteristics, Figure 6.1, an envelope of nozzle sizes which should be tested for maximum power of the jet, relating to maximum pump performance, can be calculated for a variable, constant-input driving air pressure.

The purpose of this calculation is to narrow the number of nozzle sizes to test. Earlier it was mentioned that no formula can work precisely for any jet if it is derived from another jet. However, the intent here is to find a starting place for suitable nozzle sizes to test, and to maximize the power of the jet for this application.

Figure 6.1 Manufacturer's Pump Performance Characteristics
(After Haskel Owners Manual, 1989)



By utilizing the manufacture's pump flow characteristics diagram, Figure 6.1, by using Equation 6.3 for maximum pump output, and by utilizing 0.7 for the discharge coefficient, an envelope of test nozzle sizes can be identified. Table 6.1 describes calculations for the quantity which will flow in a water jet stream for various nozzle sizes at various pump pressures that the pneumatic pump can operate at efficiently. After inspecting the pump characteristics curve, Figure 6.1, and finding the corresponding maximum output quantities at various pressures, a close approximation for the pressure range at which each nozzle size will deliver maximum pump volumes can be identified.

In Table 6.1, it can be seen that an envelope of nozzle diameters should include nozzles from 0.012 inches to 0.020 inches in diameter. It is expected that smaller nozzles will perform more efficiently at higher pump pressures, and larger-diameter nozzles will perform more efficiently at lower pump pressures. All nozzle sizes will be tested in a range of operating pressures to see if this prediction is correct.

In Table 6.1, all units on the numerical values are as follows:

Pressure: psi, Pounds per Square Inch
 Quantity: cfm, Cubic Feet per Minute
 Diameter: in, inches

Table 6.1 Quantity Versus Pressure for Various Nozzle Sizes

| | P1 | P2 | P3 | P4 | P5 |
|-----------|-------------|-------------|-------------|-------------|-------------|
| Pressure | 15,000 | 15,625 | 16,250 | 16,875 | 17,500 |
| Quantity | Q1 | Q2 | Q3 | Q4 | Q5 |
| Diameter | | | | | |
| d1 .011 | .306 | .312 | .319 | .324 | .330 |
| d2 .012 | .364 | .372 | .379 | .386 | .393 |
| d3 .013 | .427 | .436 | .445 | .453 | .461 |
| d4 .014 | .496 | .505 | .515 | .525 | <u>.535</u> |
| d5 .015 | .569 | .580 | .592 | <u>.603</u> | .614 |
| d6 .016 | .674 | .660 | <u>.673</u> | .686 | .699 |
| d7 .017 | .730 | <u>.745</u> | .760 | .775 | .789 |
| d8 .018 | <u>.819</u> | .836 | .852 | .868 | .884 |
| d9 .019 | .912 | | | | |

The underlined values identify the pressure at which each nozzle size will, in theory, deliver rated volume. The choice of nozzle sizes to test is 0.011 inches on the small side, 0.013 and 0.016 inches in the middle, and 0.019 inches on the large side.

6.3 STAND-OFF DISTANCE

Stand off distance is the distance between the orifice of the nozzle and the rock sample being cut. Perhaps the most advantageous stand off distance for mining is the largest distance which can be used while still retaining the full cutting potential of the jet. This distance is governed by the central core of the jet, which converges up to a point and then disappears, greatly reducing the cutting power of the jet. This core length is described by W.C. Cooley in terms of a ratio between the stand-off distance and the jet diameter, S / d , and a slot depth which varies inversely as the stand-off ratio, to a power usually between 0.2 and 0.4. This effect is associated with the gradual disappearance of the central core of the jet by turbulent mixing. With known diameters for testing, an optimal stand-off distance for each diameter can be calculated, and should equate to a ratio between 10, and conservatively, 55 (Cooley).

The stand-off distance does not affect the cutting of the jet in the critical region of stand-off distance, as described by Cooley. The central core of the jet is still intact in this region, and will cut equally well as long as this region is not surpassed. Therefore, the optimum stand-off distance is any distance not surpassing Cooley's critical distance.

Where:

S = Stand Off Distance
d = Nozzle Diameter
S/d = Ratio of S divided by D

Table 6.2 Stand Off Distance Suggested at Various Nozzle Sizes

| S/d | 10 | 55 | 100 |
|------|------|-------|------|
| kd | So | Sw | Sl |
| .012 | 0.12 | 0.660 | 1.20 |
| .015 | 0.15 | 0.825 | 1.50 |
| .017 | 0.17 | 0.935 | 1.70 |
| .020 | 0.20 | 1.100 | 2.00 |

It is found, when applying Cooley's equation, that the envelope for all nozzle sizes is in the order of 0.12 to 1.8 inches.

Conservative critical stand-off is less than 0.12 inches. To test the theory, a sample will be cut from zero to two inches prior to testing other parameters. Where the discrepancy of cutting is encountered, a tested critical stand-off distance will be known. The theory supported by testing in Cooley's research suggests that a critical distance should be tested for the smallest nozzle size of 0.011 inches. After this critical distance is found, all tests will be performed at a stand-off distance under the critical distance. The purpose of this will be to find the most efficient cutting power of the jet, without the stand-off distance affecting the other parameters. It is not in the intention of this thesis to find the relationship in which the stand-off distance affects the ability of the jet. This is perhaps an important relationship in a mining situation where a face is never truly smooth. However, it is beyond the scope of this research.

6.4 TRAVERSE VELOCITY

The traverse velocity of a jet is the speed at which the jet is translated across the sample being cut. For simplicity, this will be simulated by translating the rock sample across a stationary jet. In cutting, slotting, or kerfing a sample, researchers have supported the generality that, for large pressures, a slower traverse velocity will produce a deeper kerf to a critical point. However, the purpose of mining is to remove material, not necessarily to cut deep. In the breaking process, which is governed by hydrofracture and grain displacement, the greatest removal of material may be at a higher traverse velocity.

To support this argument, Conn finds that slower feed rates will produce smoother kerfs. This suggests that the roughest cut might be observed with a higher feed rate. If this is true, the greatest breaking damage per time cutting on a rock will be observed at the highest traverse velocity which still removes an appreciable amount of material.

A rodless cylinder, powered pneumatically, will be utilized to traverse samples. Four traverse velocities will be tested for each nozzle size to determine the optimum traverse velocity at optimum pressure and volume. These speeds will be between two and 20 inches per second.

6.5 EFFECT OF MATERIALS DIRECTIONAL PROPERTY

The material to be tested is Green River trona, and will be described in detail later in the thesis. Trona is a depositional deposit by origin, however, it is imbedded with many radiating crystals, having no apparent concern with the direction of the bedding plane. It will be of importance to see whether the material can be more readily removed while traversing with or against the natural bedding plane, or if it cuts more readily in a direction perpendicular to the strike

of the bedding plane. If it is found that one direction of cutting is inherently better than the other, care will be taken to cut samples in such a way as to maximize the results. Grain size, material strength, and other rock mechanics properties are important. However, it is not the intention of this thesis to compare cutting of trona with another type of material. These properties are included in the sample description, in Chapter 8.

6.6 OTHER PARAMETERS WHICH ARE NOT ADDRESSED

The effect of angle inclusion of the jet is a parameter related to the angle at which the jet hits its target. This effect will necessarily be seen in practical application as no face which is spalling can break exactly perpendicular to a jet in a ridged substance, such as rock. This effect might greatly aid in the spalling action of a particular sample. However, it will not be tested here, due to the nature of the test equipment and its limitations.

The nozzle shape and design have been extensively studied by a number of investigators. It will be assumed that commercial nozzles, made of sapphire, and relatively available and inexpensive, will be sufficient for the scope of this thesis.

CHAPTER 7

EXPERIMENTAL EQUIPMENT DESCRIPTION

All equipment utilized in this experiment has been donated by outside sources and CSM internal sources. The basic configuration of the test apparatus involves the pumping mechanism, the sample traverse cylinder and mount, water and air filter units, and a steel table on which the equipment is mounted.

7.1 PNEUMATIC INTENSIFIER PUMP

The pneumatic intensifier pump is a Haskel, Inc., Model 8 - HSF D - 225 - C, with serial number 989 - 64. It was manufactured in September, 1989. This pump is a double-acting eight horsepower pump with an output pressure range of 2,500 to 22,500 psi (pounds per square inch). The recommended pressure range for efficient pumping is 13,000 to 21,000 psi. The range of volumetric flow is between 0.3 and 0.9 gpm (gallons per minute). This particular model incorporates a high-performance eight inch bore by four inch stroke air drive section, with a large double-exhaust-ported cycling valve. This valve is unbalanced for "no hangup reliability," and is completely pilot-operated for control flexibility and positive shift without relying on springs. Drive line lubrication is not utilized. Maximum drive air pressure is 130 psi, utilizing compressed air. The pump is designed to operate at a recommended inlet water pressure of 500 psi. (Haskel, Inc., pump owners manual).

7.1.1 SCOPE OF THE INTENSIFIER PUMP

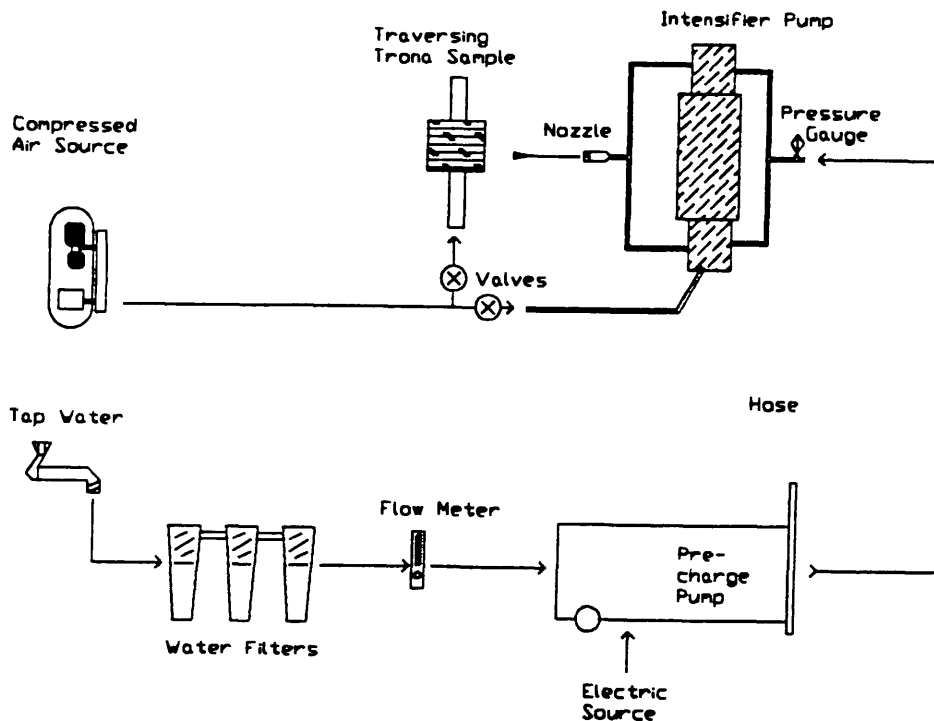
To get a clear idea of the capabilities of the pump tested, and how it fits into the realm of all water jet pumps, a table is presented showing the differences in pressures and water volumes for previously identified pumps.

Table 7.1 Comparison of Water Jet Pumps

| <u>Pump</u> | <u>Peak Pressure</u> | <u>Peak Volume</u> |
|-----------------------|----------------------|--------------------|
| Pneumatic Intensifier | 22,500 psi | 0.9 gpm |
| Hydraulic Intensifier | 40,000 to 70,000 psi | 2 - 7 gpm |
| Triplex Pump | 25,000 psi | 50 gpm |
| Hydraulic Monitor | 2,000 to 6,000 psi | 50 - 100 gpm |
| Rotary Pump | 6,000 psi | 10 - 15 gpm |

The experimental pneumatic intensifier that is tested has a very low peak volume and medium-high pressure. With the pneumatic intensifier to be tested, a certain challenge exists. The amount of work needed to run an air compressor large enough for driving this type of pump exceeds the work requirements for most other water jets. There is much promise, however, in the relationship between pressure and volume delivered by the pump to be tested. Other pumps exist that can provide similar relationships more economically, such as very small hydraulic intensifiers and triplex piston pumps with very small piston diameters and large strokes.

Figure 7.1 Schematic diagram of test facilities



7.2 HIGH PRESSURE CONNECTIONS

All high pressure connections exceed maximum working load specifications. These are a combination of Autoclave-brand and equivalent Butech-brand fittings.

7.3 NOZZLE CONFIGURATION AND DESIGN

The nozzles used are sapphire (calcium silicate) nozzles imbedded into a machined stainless steel (type 316) reservoir type nozzle mount utilizing the older O-ring type seal (newer types utilize wax and no O-ring). The small, high-pressure reservoir is approximately 1.5 cubic inches, and aids in the

delivery of a smooth, continuous jet. This creates a longer core length of the jet, resulting in a longer critical cutting length of the jet stream. The nozzles are of Leach and Walker styling, and incorporate a 13 degree conical shape from centerline of the nozzle to the conical edge of the nozzle. The conical opening is followed by a straight section greater than the length of the conical section axially. The nozzle is fed by both sides of the double-acting intensifier pump by 1/8 inch id (inside diameter), 3/8 inch od (outside diameter) high-pressure, seamless stainless steel tubing.

7.4 FEED PUMP

The intensifier pump is pre-charged with an electric-driven centrifugal feed pump. This pump, originally set up for common pressure washing, delivers 500 psi pressure at approximately two gpm. This pump is set in line, after the filter unit and before the intensifier pump.

7.5 AIR FILTER UNIT

This filter is an Airline, Co., Series F3 metal-bowed filter, with maximum pressure of 250 psi and temperature range up to 200 degrees Fahrenheit.

7.6 WATER FILTER UNIT

This filter unit is a series of three Teel Water Systems, Inc., Model 2P275 filters. These filters will remove all particulate and deionize the water to a degree of .00001 inch particles. Internal filters can be exchanged after use for ease of maintenance.

7.7 RODLESS CYLINDER TRAVERSE MECHANISM

A rodless cylinder is used for traversing the sample across the jet. The cylinder used is an SLR - MOO Model 32 cylinder. It is powered by up to 20 psi of air, which can be adjusted with an electric actuator switch to traverse speeds from zero to 20 inches per second, with or without a load. The stroke of this particular cylinder is 12 inches, with approximately one inch of acceleration and one inch of deceleration within the 12 inch stroke. The cylinder is connected to a double actuator which allows it to operate equally well in either direction. The actuator is fully adjustable, and allows for changes of constant velocity speed in either direction, independently.

7.8 SAMPLE SUPPORT ON CYLINDER

The support for the rock sample is a one square foot lexan plate, bolted to the cylinder mount directly in the center of the plate. The plate is supported by four two-inch casters, mounted on the four corners of the plate to avoid overloading of the cylinder.

7.9 TRAVERSE VELOCITY INSTRUMENTATION

A mechanical switch wired to a digital stop watch is tripped at an eight inch interval by the casters of the lexan plate support as the cylinder traverses at constant velocity past the switch. As the traverse is made, the switch automatically starts and stops the stop watch. With the known eight inch interval and time for the traverse, a traverse velocity can be calculated.

7.10 STEEL TABLE

The steel table on which the testing apparatus is mounted is constructed of I - beams and a steel plate. Four inch by three inch I - beams serve as legs, and are welded to a 1/4 inch table top at a three foot height. A 1/4 inch supportive steel plate is welded under the tabletop one foot from the floor, and serves as a storage shelf. The tabletop and shelf are supported by three inch and two inch angle iron, respectively, and surround both surface circumferences. Overall dimensions of the table are three-feet-high by four-feet-wide by six-feet-long. The weight of the table serves as a suitable mount for the pneumatic pump, without which the pump would jump violently.

7.11 SAFETY SHIELD

A safety shield is constructed of 1/4 inch plexiglass, and encompasses the entire cutting test area of the water jet. The plexiglass is a box on both sides, in front of the line of fire and on top of the jet. This leaves the only exposed area behind the high pressure pump.

CHAPTER 8

SAMPLE MATERIAL TESTED

The material tested with the water jet assembled for this thesis is naturally-occurring trona, currently mined in Green River, Wyoming. The complex nature of the formation of trona warrants a brief geologic description of the deposit nature and depositional setting. Several seams of trona are currently mined in the Green River Basin. The trona mined occurs at different depths. Associated with these depths, different brittleness and crystallinity occurs within the total deposit. The trona tested in this thesis comes from Tg Soda Ash, Inc.

8.1 FORMATION OF THE TRONA DEPOSITS

The Green River Basin is a large, synclinal basin and is a result of the Eocene epoch. Early in the Tertiary period, the floors of the basins in the area down-warped, causing continuous sedimentation of the Green River Basin.

This basin is in the shape of a lens, or pile of lenses, embedded in an enormous volume of sediments. The Green River Basin has been divided into three known members corresponding to three different depositional settings. These settings correspond to the changing of a large lake, Lake Gosiute, over a period of about four million years during the Green River epoch. (Bradley)

Of these three stages, the first and the third correspond to a humid environment, when Lake Gosiute was very large and had an opening. The second stage corresponds to a more arid environment, which shrank to about half of its former size and presented the water with no opening for flow. As a result, very saline conditions prevailed. These conditions were just

right for the deposition of trona.

This second stage of the ancient lake produced immense deposits totalling over 100 billion tons of bedded trona. At least 42 beds of trona, in an area of about 1300 square miles, exist at depths ranging from about 400 to 3500 feet.

The major beds, those that are three feet and greater in thickness, are numbered by Bradley, Eugster, and Culbertson, from one to 25, and underlie an area of at least 100 square miles. The thickness of these beds are as much as 37 feet (Bed 1), and they underlie an area of up to 350 square miles (Bed 17). The remaining 17 minor beds range in maximum thickness from one to four feet, and underlie from as little as 10 to as much as 400 square miles. (Culbertson) The mined trona beds are similar in most aspects, particularly in grade and thickness, but some differences do exist. Trona Bed 17 is notably consistent in grade and appearance, and is relatively fine-grained throughout and uniformly tan in color, with inconspicuous shale layers. Alteration and recrystallization in this bed appear to have been minor. Beds 19 and 20 resemble beds 24 and 25 in crystallinity and evidence of solution activity and recrystallization. Coarse trona with rosettes, radiating sheaves of crystals, are dominant in beds 19, 20, 24, and 25, although finer-grained trona is present. The coarse trona found in these beds is more brittle than that found in the other beds (Deardorff and Mannion). This is an important feature of the trona tested in this thesis, as the tested trona comes from the coarser, more brittle crystallized trona of Bed 20.

8.2 SAMPLE DESCRIPTION

Tg Soda Ash, Inc., trona comes from bed 20, which is currently mined at a depth of 1450 feet. The mining methods

used for this bed are predominantly continuous, utilizing room and pillar, and for a time, short wall mining. Both methods involve the use of continuous miners.

The samples used for this thesis were cut from approximately 1.5 to two cubic foot cubes, donated by the mining company solely for the purpose of this experiment. These samples are cut into bricks ranging from five to seven inches long, four to five inches high, and two to four inches wide. These samples were cut following preliminary testing to determine the effect of the bedding plane of the sample on the cutting jet.

Uniaxial compressive Strength of the sample was measured at 5840 psi. for three samples tested. Dr. John F. Abel, Professor of Mining Engineering, CSM, found a compressive strength of 5710 psi. for 42 samples tested. Density of trona ranges between 78 and 82 pounds per cubic foot. All calculations based on the density use a density factor of 80 pounds per cubic foot. Porosity, permeability, and grain size varies greatly within the sample due to the extent of the crystallinity. Although these factors are very important in the fracturability of the trona, no data could be found for these values in the scope of this thesis.

CHAPTER 9 TESTING PROCEDURES

Testing procedures include the optimization of water jet parameters as described in the statement of thesis intent, Chapter Five. This optimization includes two main subdivisions of testing: optimization of parameters involving pump-specific items, including the performance of the water jet; and, optimization of parameters involving the test sample. Table 9.1 is a list of identified parameters to be tested. Pump dependent parameters are those parameters which change performance of the water jet alone, and sample dependent parameters are parameters which effect the cutting ability of the water jet.

Table 9.1 Identified Testing Parameters

1. Pump Dependent Parameters
 - A. Volume-to-Pressure Ratio
 - a. Input Driving Air Pressure
 - b. Water Volume Delivered vs. Nozzle Size
 - c. Pressure delivered vs. Nozzle Size
2. Sample Dependent Parameters
 - A. Stand-Off Distance
 - B. Geometry of Sample
 - C. Traverse Velocity

9.1 TESTING PROCEDURE FOR PUMP DEPENDENT PARAMETERS

An eight horsepower pneumatically-driven intensifier pump is powered by a 400-cfm air compressor. This pump could conceivably be run with a much smaller compressor. However, a very large compressor was used so that the limits of the compressor would not effect the true performance of the pump.

The intensifier pump will perform at different levels, depending on the following parameters:

Input Driving Air Pressure: 75 - 115 psi.
Output Water Volume: 0.3 - 0.9 cfm.
Output Water Pressure: 5,000 - 35,000 psi.

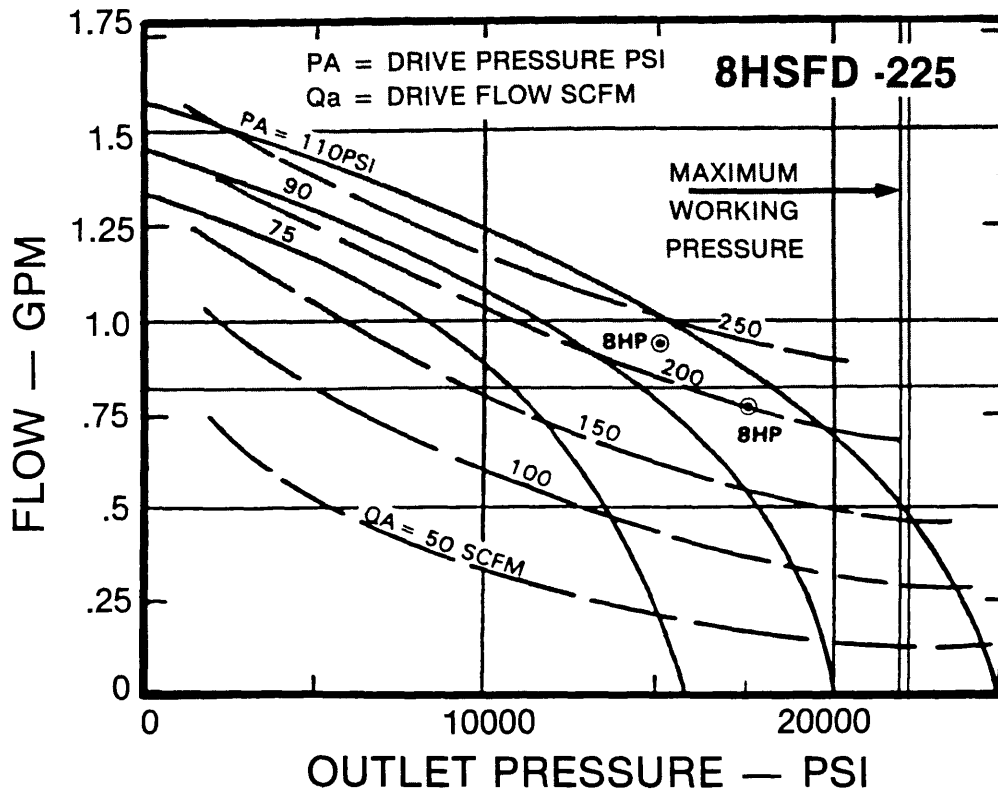
Figure 9.1 is the manufacturer's pump performance curve, which is shown on the following page. Controlling parameters for pump performance identified are:

1. Nozzle Size
2. Input Driving Air Pressure
3. Input Driving Air Quantity

Of these, only the nozzle size and the input driving air pressure can be varied. The pump will take as much driving air quantity as its eight inch piston by four inch stroke will handle. The pump was tested with a 120-cfm compressor and the results were significantly worse than those found when using the 400-cfm compressor. With the 400-cfm compressor, the air is completely unconfined. Therefore, this parameter was not used to vary the output water quantities and pressures at different nozzle sizes.

Water quantity delivered for various input-driving air pressures for specific nozzle sizes can also be measured. This parameter is measured using a flow meter on the low pressure side of the pump. With negligible losses, Bernoulli's principle for flow dictates that the quantity of water that goes into the low pressure side of the intensifier pump must be delivered out of the high pressure side of the pump at the same flow rate.

Figure 9.1 Manufacturer's Pump Performance Characteristics
(After Haskel Owners Manual, 1989)



The water is assumed to be compressible at the nozzle orifice, however, when it reaches the point of impact on the water jet target, it will have expanded to its original state and thus will flow at the same rate. The other argument which could be addressed is that when the water is pressurized into the water jet, it behaves as a three-phase flow, liquid water, air-with-water mixture, and gaseous water. Some of the water which escapes through the nozzle will not aid in the breakage of rock, as it is in the form of this air/water and gaseous

state, and expands conically outward from the main stream of the water jet. However, the same amount of water is still flowing on the low side of the pump as on the high-pressure side, and it is assumed that the total volume flowing is the quantity with which the pump is performing, regardless of the compressibility factor and the water losses in the jet stream.

Input driving air pressure can be measured, and is the controlling variable, since it can be readily varied by hand and directly read off of a meter as it enters into the pump.

Output water pressure could be measured using a high-pressure water gauge on the reservoir of the nozzle chamber. This parameter can also be found with the manufacturer's pump characteristics curve, Figure 9.1, using the known input driving air pressure and the output water volume.

For each nozzle size tested, the following procedure is used to determine output water pressure delivered at specific input driving air pressures. Given a particular nozzle size:

- 1) Vary the input driving air pressure from the highest to the lowest possible value, using increments of five psi. This is approximately from 115 to 75 psi, depending on the nozzle;
- 2) For each pressure, measure the input water quantity flowing and record both values;
- 3) Repeat the above procedure for three repetitions;
- 4) Average the three values of water quantity for the three repetitions, and read and record the output water pressure for each quantity at perspective input driving air pressures. This value is found on the manufacturer's pump characteristic curve; and,
- 5) Determine, using calculations previously shown in the scope of this thesis to find the pressure for each nozzle size and quantity delivered. Use these for comparative rock cutting tests.

The pressures used for comparison range between 5000 and 35,000 psi depending on the nozzle size.

9.2 TESTING PROCEDURES FOR SAMPLE PARAMETERS

Initial testing procedures will determine the maximum stand-off distance for testing inside of the critical cutting region of the water jet, and the best geometry placement of the sample. Each test will utilize a 0.015 inch diameter nozzle size and a pressure of 17,000 psi. Testing procedures are as follows:

9.2.1 STAND-OFF DISTANCE

- 1) Traverse a sample sitting at a 10 degree angle to the perpendicular of the jet. One side of the sample is directly at the nozzle orifice with the other side exactly at one inch from the nozzle orifice. The sample is six inches long;
- 2) Measure the width, depth, and volume of the cut at 0.25 inch intervals;
- 3) Repeat the above procedure for three repetitions on four separate samples, varying the traverse velocity for each sample tested; and,
- 4) Compare the results to see if a trend is found.

9.2.2 DIRECTIONAL PROPERTY OF SAMPLE

- 1) Traverse a sample parallel to the sample's natural bedding plane using three repetitions;
- 2) Traverse a sample perpendicular to the sample's natural bedding plane using three repetitions;

- 3) Traverse a sample perpendicular to the strike of the sample's natural bedding plane using three repetitions; and,
- 4) Compare results for depth, width, and volume to see which geometry is more readily cut with the water jet.

9.2.3 TRAVERSE VELOCITY

Traverse velocity will be varied by physically adjusting the rodless cylinder and measuring the time it takes to reach from one set point to another. The time is measured for each sample and is optimized to exact traverse velocities using the following procedure:

- 1) Place a trona sample on the lexan traverse plate and secure it;
- 2) Hold the mechanical switch connected to the stop watch in line with the idler on the lexan plate;
- 3) Trip the switch to start the traverse of the rodless cylinder supporting the plate;
- 4) Hold the mechanical switch in line with the front and back idler, so that the front idler starts the stop watch and the back idler stops the stop watch;
- 5) Read the stop watch and adjust the cylinder to a faster or slower position using a screw driver;
- 6) Repeat the procedure until the time is exactly within .01 seconds to ensure the exact traverse velocity as the one desired; and,
- 7) Run the test one more time to ensure accuracy.

When the desired traverse velocity is set to the correct

speed, a test can be performed for each of three pressures. Traverse velocities tested for every nozzle size and for each pressure setting are 2, 6, 12, and 20 inches per second.

9.2.4 WATER JET PRESSURE

For each nozzle size, optimal input driving air pressures are calculated for achieving three or four output water pressures, for each of the nozzle sizes. The procedure for testing each sample for pressure begins at the start of each repetition in the traverse velocity procedures, so that all pressures tested for all nozzle sizes are tested for all traverse velocities.

- 1) Turn on the water jet to the prescribed input driving air pressure corresponding to the desired output water pressure;
- 2) Trip the switch to start the traverse of the sample across the water jet;
- 3) Repeat this procedure for three repetitions for the desired pressure; and,
- 4) Adjust the traverse velocity to the next corresponding speed and repeat the above procedure for all of the pressures.

9.2.5 NOZZLE SIZE

This parameter is varied by changing nozzle sizes and repeating all of the previous testing procedures.

9.3 MEASURING WATER JET PERFORMANCE

Water jet performance is measured for each cut made in a trona sample. The three measurements taken are the depth, the apparent width, and the volume of removal. Because of the pump's nature, the greatest impact is made in the middle of a pump stroke. When one stroke of the reciprocating piston is beginning, and one is ending, the jet loses pressure for a fraction of a second. It was necessary to take the best two inch section observed on each sample traverse to ensure the accuracy of the volume-to-pressure ratio the pump can deliver. Recall that the goal of this thesis is to find the rate at which this ratio can cut, not necessarily the performance of the particular pump used.

On some samples the optimum two inch section occurred directly in the middle of the sample, and on some it was observed on one end or the other. Samples used were five to six inches in length so that a guaranteed best cut, or one occurring in the middle of the pump stroke, could be observed on every sample tested.

9.3.1 DEPTH OF CUT

The depth of cut was found using a wire of 0.005 inch diameter, and by following the procedures:

- 1) Identify the best two inch section observed on the trona sample kerf to be measured and mark this;
- 2) Insert the wire into the sample at one mark until it reaches the depth of the kerf. Pinch the exact location of the wire where it is flush with the surface of the sample with fingernails;
- 3) Take the wire and measure the distance between the pinch and the end of the wire on a scale. This is measured and recorded in millimeters;
- 4) Repeat this procedure for four random locations

within the two inch interval approximately every 1/2 inch; and,

- 5) Average the four measurements for average depth.

9.3.2 APPARENT WIDTH

A scale in millimeters is used to measure the widest and the thinnest section of the identified two inch region. The median of these two measurements is used to determine the apparent width of the kerf.

9.3.3 VOLUME OF THE KERF

The volume was found using a putty substance, known commercially as Play-Doh brand modeling compound. A perfect one cubic centimeter cube was molded out of the material, and was displaced in a graduated cylinder full of water to see if it would accurately displace water for a volumetric measurement. This proved to be the case for three samples tested, so it was assumed that this was an accurate method for measurement. The following procedure was used to measure the volume of the identified two inch section on each sample kerf.

- 1) Pack putty into the identified two inch section on sample kerf until it is flush with the sample surface;
- 2) Using a wire extract the putty and form it into a ball;
- 3) Drop the putty ball into a graduated cylinder filled partially with water to measure the volume displaced. A 10 cc graduated cylinder filled with water to exactly four cc was used in

every case; and,

- 4) Record the volumetric displacement for the two inch section tested.

9.3.4 RATE OF REMOVAL

The rate of volumetric removal can be found by multiplying the volume removed per two inch section with the traverse velocity, and is seen in the data as the rate of removal with units of cubic centimeters removed per second.

CHAPTER 10
EXPERIMENTAL RESULTS

Experimental results are shown for the pump parameters and the sample parameters. A copy of all the sample data is included in the Appendix.

10.1 PUMP DEPENDENT PARAMETERS

Table 10.1 shows the theoretical pressures calculated using bernoulli's equation and the continuity equation, given tested nozzle sizes and measured volume outputs for specific input driving air pressures. Calculations for specific water jet powers and respective pump efficiencies are included.

Table 10.1 Pressures Achieved for Flow Rates Through Specific Nozzle Sizes.

| Nozzle Size in. | Water Volume gph. | Water Pressure psi. | Jet Power hp. |
|-----------------------|-------------------------|---------------------------|---------------------|
| 0.011 | 28 | 34,600 | 13.46 |
| | 27 | 32,200 | 12.07 |
| | 23 | 23,500 | 7.50 |
| | 18 | 14,600 | 3.67 |
| 0.013 | 33 | 24,800 | 11.37 |
| | 31 | 21,900 | 9.43 |
| | 28 | 18,000 | 7.00 |
| | 24 | 13,300 | 4.43 |
| 0.016 | 39 | 15,300 | 8.29 |
| | 35 | 12,400 | 6.03 |
| | 29 | 8,700 | 3.50 |
| 0.019 | 52 | 13,700 | 9.90 |
| | 46 | 10,800 | 6.90 |
| | 35 | 6,500 | 3.16 |

Each nozzle size tested displays a different performance level for pressures, jet powers, and pump efficiency achieved. All nozzles display a general trend of producing higher pressures at higher respective water volumes. Also observed, is a trend for better pump efficiencies at higher jet horse powers, corresponding to larger jet pressures achieved. As expected, smaller nozzle sizes produce higher respective pressures at relatively lower volumes. The smallest nozzle size produces a pump efficiency over 100 percent. This is due to a horse power output which is larger than the rated horse power of the pump. In the results that follow, it is interesting to find that jets with larger pressures do not necessarily produce better trona cutting action.

10.2 STAND-OFF DISTANCE

In this test a sample was passed with a varying stand-off distance from zero to one inch. The data displayed no difference in performance between the zero to one inch section. It was predicted earlier that for any material, and depending on the material, a difference could be found between the values of 0.14 inches and 1.5 inches. Apparently, the trona sample is so readily kerfed that within one inch of stand-off distance, the jet is still within range of the critical zone of cutting. The decision was made to pass each sample across the jet at the closest location to the orifice of the jet as possible. Since the samples were smooth but not polished, this location was in the range of less than 1/2 inch, and varied slightly, depending on the contour of the sample. In this range of stand-off distance, with the advent of the stand-off test, it is assumed that the distance used did not limit the ability of the jet.

10.3 GEOMETRY OF THE SAMPLE

The geometry of the sample is not clearly defined in terms of jet performance. In the trona sample tested, the bedding plane was, at best, only identified in scattered places. Most of the samples had rosettes, radiating crystals expanding through the sample, and, in some cases, expanding throughout the entire sample. Even when the bedding plane was recognized, it was not a smooth plane. It was more or less a band of highly wrinkled, inconsistent evidence of deformation. When tested, it was found that the bedding plane did not make any significant difference in the performance of the jet. What did make a difference was the radiating crystals, which, when cut, appeared to spall more readily than the finer grained portions of the samples tested for geometric positioning.

It was decided, due to support in the literature of testing done on Wikenson Sandstone (McClain), to use a geometry perpendicular to the bedding plane for testing. All samples were cut so that the jet could be passed perpendicular to the bedding plane for consistency. This was accomplished by cutting samples with two planes parallel to the bedding plane so that four planes were perpendicular to the bedding plane and could be tested.

10.4 SAMPLE PARAMETER DATA

The results of the samples tested are shown in detail in the Appendix. Tables of the averages of all data for each nozzle size are shown in Tables 10.2 - 10.5. Table 10.2 displays volume removal at specific traverse velocities for each nozzle size at various pressures achieved. Table 10.3 displays the apparent widths achieved, Table 10.4 displays the

kerf depths achieved, and Table 10.5 displays the cutting rates achieved, for the above respective parameters. Table 10.6 displays the specific energy data calculated for the cutting rates achieved at various jet powers and pump efficiencies.

Table 10.2 Volume of Trona Removed for Various Nozzle Sizes

| Nozzle Size in. | Water Pressure psi. | Volume Removed Per Two Inch Kerf, cu cm. | | | |
|---------------------------|-------------------------------|--|------|------|------|
| | | Traverse Velocity, in / sec | | | |
| | | 2 | 6 | 12 | 20 |
| 0.011 | 34,600 | 1.40 | 0.67 | 0.87 | 0.53 |
| | 32,200 | 1.67 | 1.03 | 1.00 | 0.20 |
| | 23,500 | 1.89 | 1.12 | 1.07 | 0.16 |
| | 14,600 | 2.13 | 0.87 | 0.90 | 0.10 |
| 0.013 | 24,800 | 1.77 | 1.43 | 1.17 | 0.60 |
| | 21,900 | 1.20 | 0.93 | 0.87 | 0.23 |
| | 18,000 | 1.30 | 1.01 | 0.64 | 0.15 |
| | 13,300 | 1.23 | 0.90 | 0.33 | 0.00 |
| 0.016 | 15,300 | 1.47 | 1.27 | 1.03 | 0.37 |
| | 12,400 | 1.77 | 1.07 | 0.80 | 0.23 |
| | 8,700 | 0.73 | 0.67 | 0.40 | 0.00 |
| 0.019 | 13,700 | 1.33 | 1.13 | 0.33 | 0.00 |
| | 10,800 | 1.27 | 0.23 | 0.00 | 0.00 |
| | 6,500 | 0.27 | 0.00 | 0.00 | 0.00 |

Table 10.3 Apparent Widths Achieved for Various Nozzle Sizes

| Nozzle Size in. | Water Pressure psi. | Average Width of Two Inch Kerf, mm. | | | |
|---------------------------|-------------------------------|-------------------------------------|------|------|------|
| | | Traverse Velocity, in / sec | | | |
| | | 2 | 6 | 12 | 20 |
| 0.011 | 34,600 | 6.33 | 5.00 | 4.67 | 5.00 |
| | 32,200 | 9.00 | 5.17 | 4.67 | 2.17 |
| | 23,500 | 7.60 | 6.67 | 5.00 | 1.50 |
| | 14,600 | 9.50 | 7.17 | 6.50 | 0.83 |
| 0.013 | 24,800 | 6.00 | 6.83 | 7.33 | 5.33 |
| | 21,900 | 4.50 | 3.33 | 3.67 | 1.83 |
| | 18,000 | 7.50 | 4.50 | 4.00 | 1.25 |
| | 13,300 | 9.17 | 5.17 | 3.50 | 0.00 |
| 0.016 | 15,300 | 7.60 | 7.17 | 6.83 | 6.50 |
| | 12,400 | 10.17 | 6.50 | 6.83 | 3.17 |
| | 8,700 | 7.00 | 6.17 | 4.00 | 0.00 |
| 0.019 | 13,700 | 6.50 | 6.50 | 3.67 | 0.00 |
| | 10,800 | 5.50 | 2.33 | 0.00 | 0.00 |
| | 6,500 | 3.00 | 0.00 | 0.00 | 0.00 |

Table 10.5 Cutting Rates Achieved for Various Nozzle Sizes

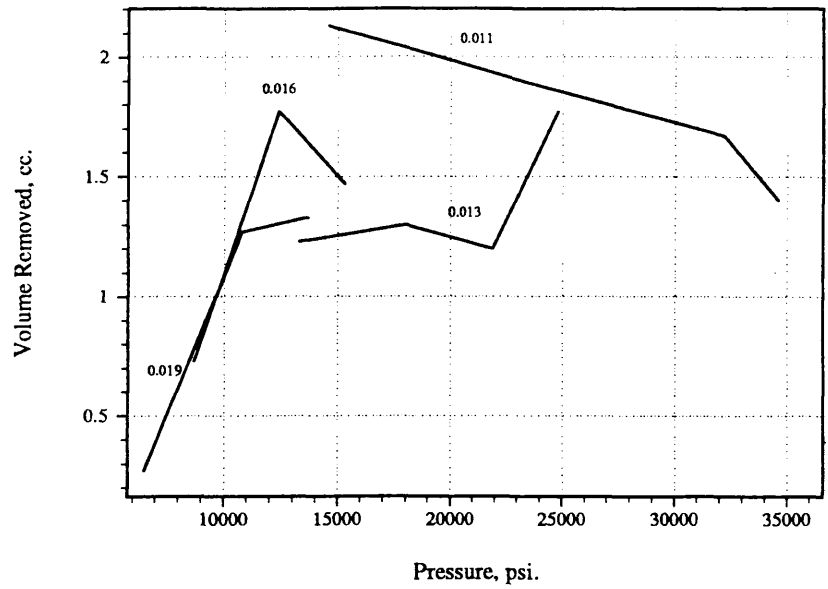
| Nozzle Size | Water Pressure | Cutting Rate Achieved, cu cm./ sec. | | | |
|----------------|-------------------|-------------------------------------|-------|-------|-------|
| | | ----- | | | |
| in. | psi. | ----- | | | |
| | | Traverse Velocity, in / sec | | | |
| | | 2 | 6 | 12 | 20 |
| | | ----- | ----- | ----- | ----- |
| 0.011 | 34,600 | 1.40 | 2.81 | 5.22 | 5.30 |
| | 32,200 | 1.67 | 3.09 | 6.00 | 2.00 |
| | 23,500 | 1.89 | 3.36 | 6.42 | 1.60 |
| | 14,600 | 2.13 | 2.61 | 5.40 | 1.00 |
| 0.013 | 24,800 | 1.77 | 4.29 | 7.02 | 6.00 |
| | 21,900 | 1.20 | 2.79 | 5.22 | 2.30 |
| | 18,000 | 1.30 | 3.03 | 3.84 | 1.50 |
| | 13,300 | 1.23 | 2.70 | 1.98 | 0.00 |
| 0.016 | 15,300 | 1.47 | 3.81 | 6.18 | 3.70 |
| | 12,400 | 1.77 | 3.21 | 4.80 | 2.30 |
| | 8,700 | 0.73 | 2.01 | 2.40 | 0.00 |
| 0.019 | 13,700 | 1.33 | 3.39 | 1.98 | 0.00 |
| | 10,800 | 1.27 | 0.69 | 0.00 | 0.00 |
| | 6,500 | 0.27 | 0.00 | 0.00 | 0.00 |

In the original testing procedure, only three nozzle sizes were tested. These were 0.013, 0.016, and 0.019 inches. This was due to the initial calculations performed to determine the nozzle size. After graphing the data, it was found that the results were decreasingly favorable from the 0.013 inch to the 0.019 inch nozzle size. It was determined that a fourth nozzle size, the 0.011 inch size, should be tested to see whether it produced even more favorable results than the 0.015 inch size. If it did, then another nozzle would have been tested until an optimum size was found. After a look at all of the graphs, an explanation of the findings will be presented.

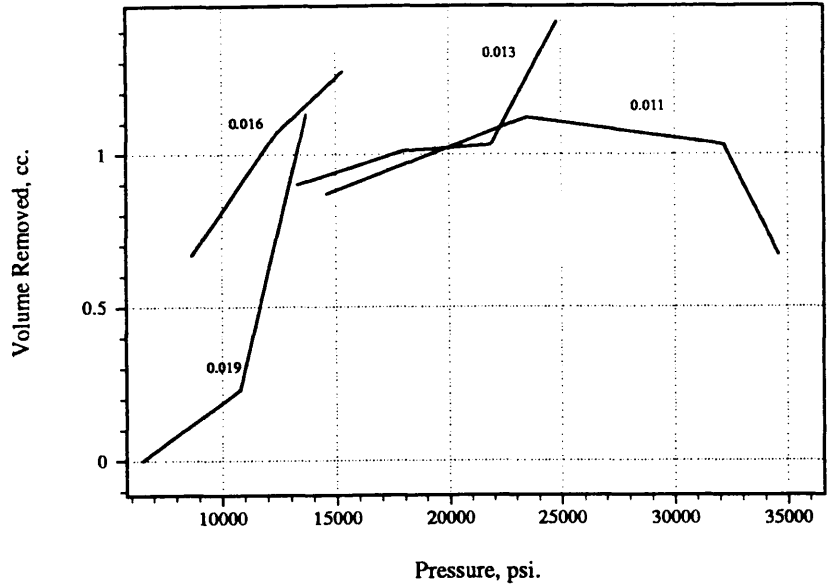
Graphs 10.1, 10.2, 10.3, and 10.4 show the results of the volumetric removal, for a two inch traverse, in cubic centimeters at various pressures for each nozzle size. Each graph corresponds to traverse velocities with ranges of two inches per second, six inches per second, 12 inches per second, and 20 inches per second, respectfully.

Definite trends can be established for generalities found in the graphs. Although each nozzle displays different peak pressures, higher volumetric removals are observed at larger pressures up to about 25,000 psi., and then tapering off from there. In general, higher volumetric removals are observed at lower traverse velocities. Keeping in mind that a higher volumetric removal at a lower traverse velocity may not produce optimal cutting rates, a look at further graphs is necessary.

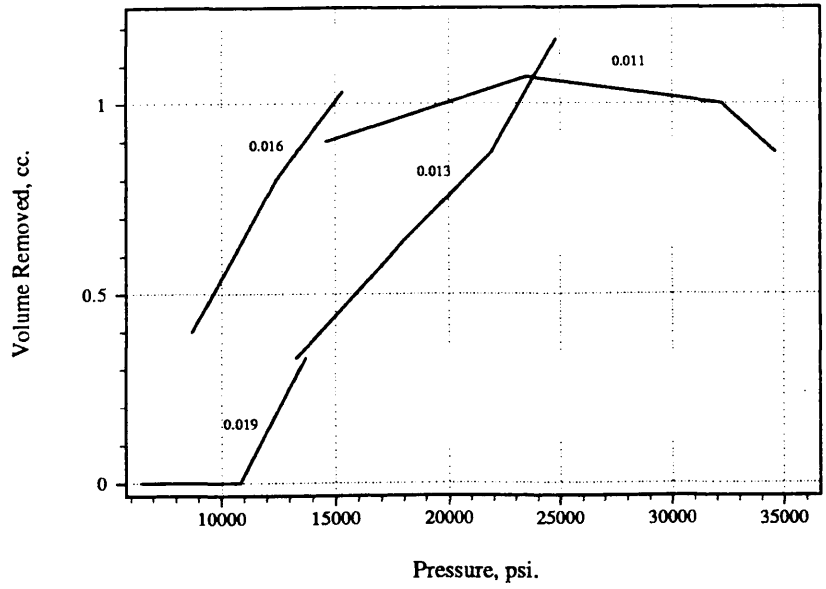
Graph 10.1 Volume Removed vs. Pressure at Traverse Velocity 2 in/sec. for Various Nozzle Sizes



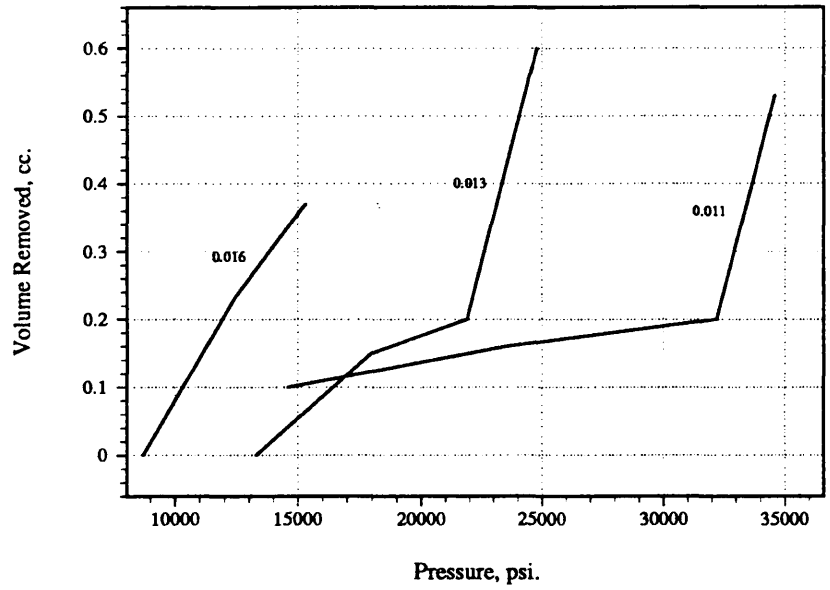
Graph 10.2 Volume Removed vs. Pressure at Traverse Velocity 6 in/sec. for Various Nozzle Sizes



Graph 10.3 Volume Removed vs. Pressure at Traverse Velocity 12 in/sec. for Various Nozzle Sizes

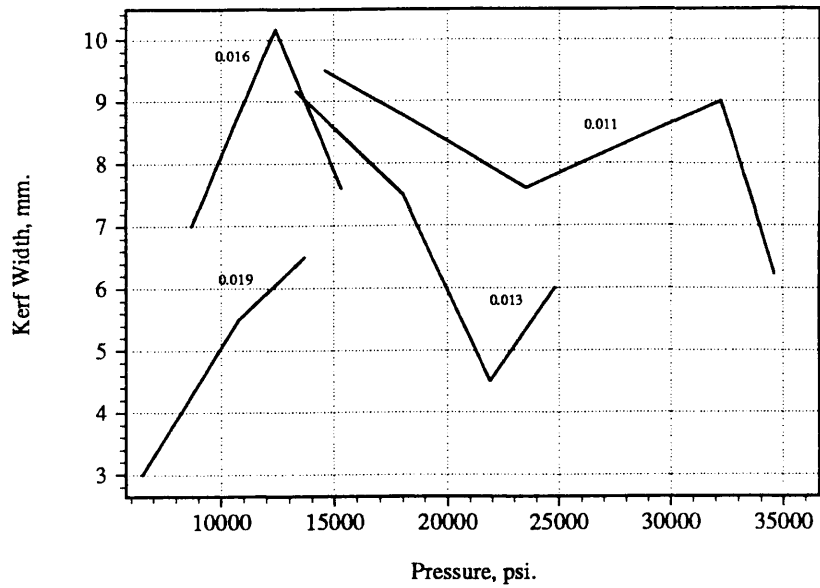


Graph 10.4 Volume Removed vs. Pressure at Traverse Velocity 20 in/sec. for Various Nozzle Sizes

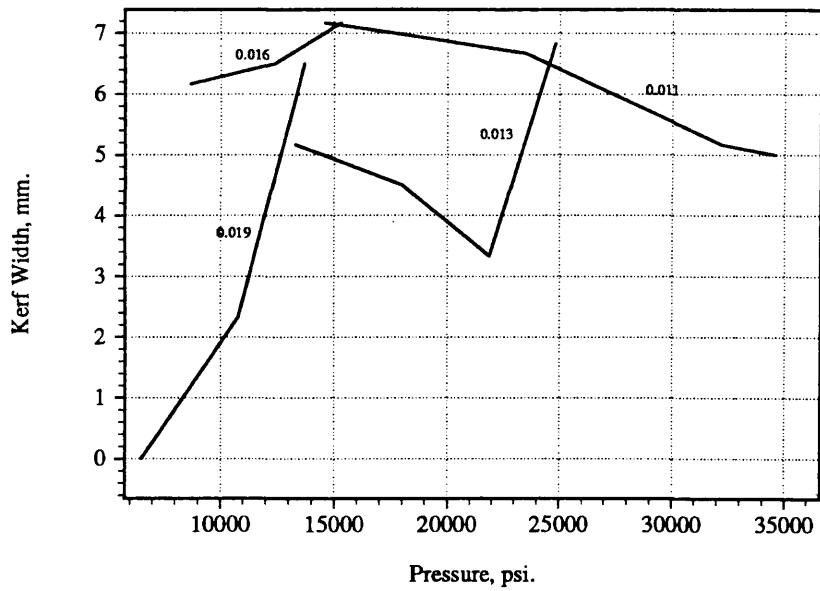


Graphs 10.5, 10.6, 10.7, and 10.8 display the apparent kerf width achieved for each traverse velocity, graphed respectfully, plotted against the range of pressures tested, for each nozzle size. These graphs are perhaps the most challenging, of the group, to decipher. General trends can be established, however, in determining the behavior of the water jet at various pressures. In the slowest three traverse velocities, kerf width advances in size up to a pressure of about 15,000 psi., and then tapering off from there. This is supported in the literature, as larger pressures are traditionally associated with greater depth, and smaller, or cleaner kerf widths, in a variety of materials. In the case of rock, many tests have found larger kerf widths, associated with larger volumetric removals, at lower pressures. For the data found in this thesis, the smaller nozzle sizes produce larger pressures, and therefor have a trend of decreasing kerf width with increasing pressures. The larger nozzle sizes, on the other hand, tend to increase in kerf width with increasing pressures. This could be associated with the larger jet diameters, which might not produce granular displacement as well as the smaller nozzle sizes. Therefor, the large kerf widths are associated with global fracture based failure, due to micro fracturing along the crystal boundaries rather than simple individual grain displacement. In support of this argument, in the next set of graphs, displaying the kerf depth, it would be expected to see a trend of increasing depth, at higher pressures, with decreasing nozzle sizes.

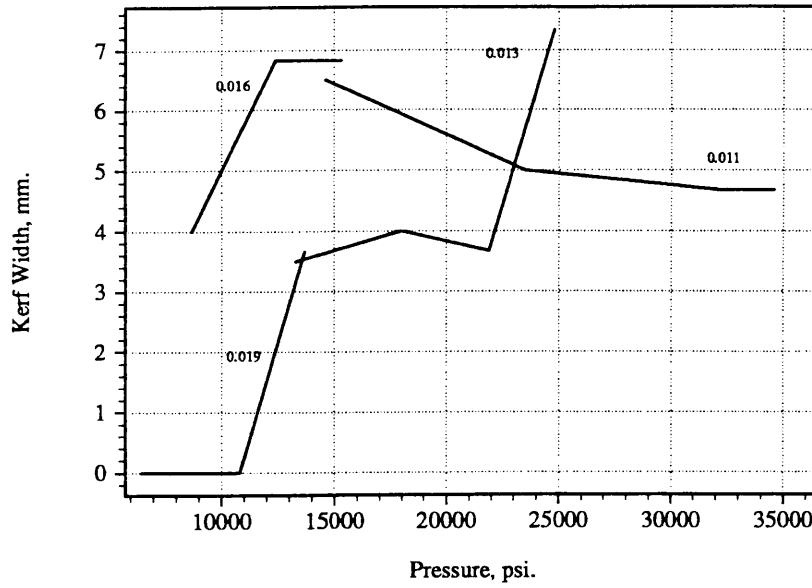
Graph 10.5 Kerf Width vs. Pressure at Traverse Velocity of 2 in/sec. for Various Nozzle Sizes



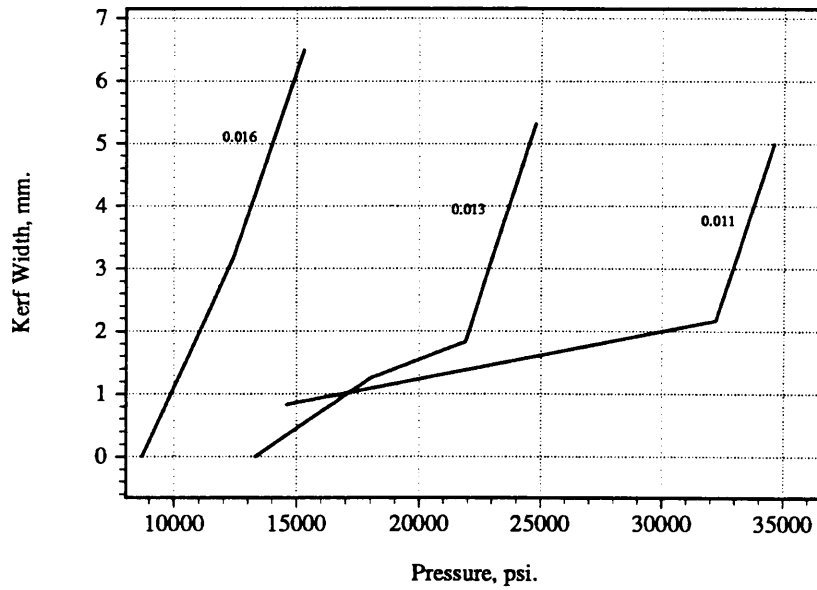
Graph 10.6 Kerf Width vs. Pressure at Traverse Velocity of 6 in/sec. for Various Nozzle Sizes



Graph 10.7 Kerf Width vs. Pressure at Traverse Velocity of 12 in/sec. for Various Nozzle Sizes

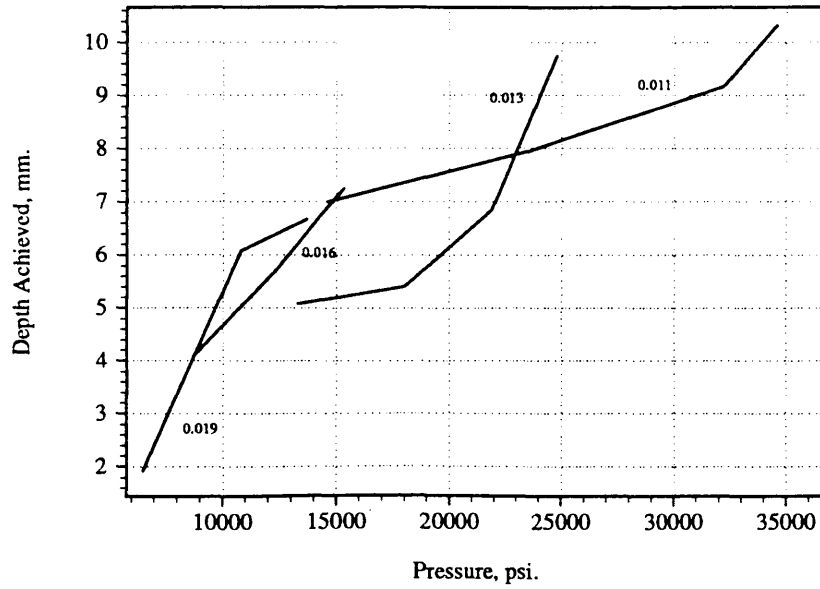


Graph 10.8 Kerf Width vs. Pressure at Traverse Velocity of 20 in/sec. for Various Nozzle Sizes

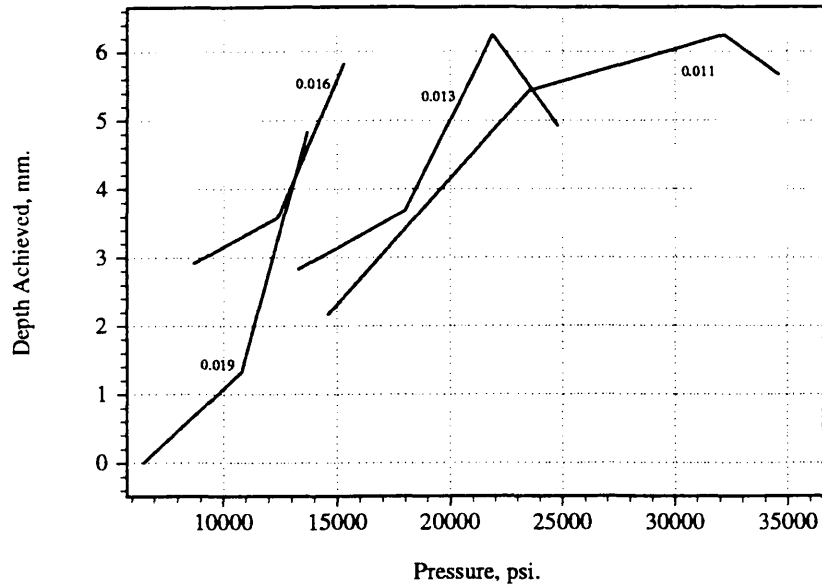


Graphs 10.9, 10.10, 10.11, and 10.12 display the average kerf depth achieved for each respective traverse velocity, plotted against various pressures, for each nozzle size. As was expected, a general trend can be established for greater depths achieved at greater pressures. All nozzle sizes follow this trend and these graphs display this very readily. As traverse velocity increases, the depth achieved tends to decrease. This is expected, as the water jet does not have the same amount of time to act on individual grains, associated with achieving depth. In the literature, all materials tested react similarly to this phenomenon. As pointed out earlier, achievement of depth is not the focus of this thesis, as this does not determine ultimate cutting ability of material in the mining sense. The object of this thesis is to remove material which is a function of depth achieved, width achieved, and ultimately the volume removed in a specific time frame, with a specific amount of energy. In the graphs that follow, the cutting rate, associated with the volume removal in specific time frames, is investigated.

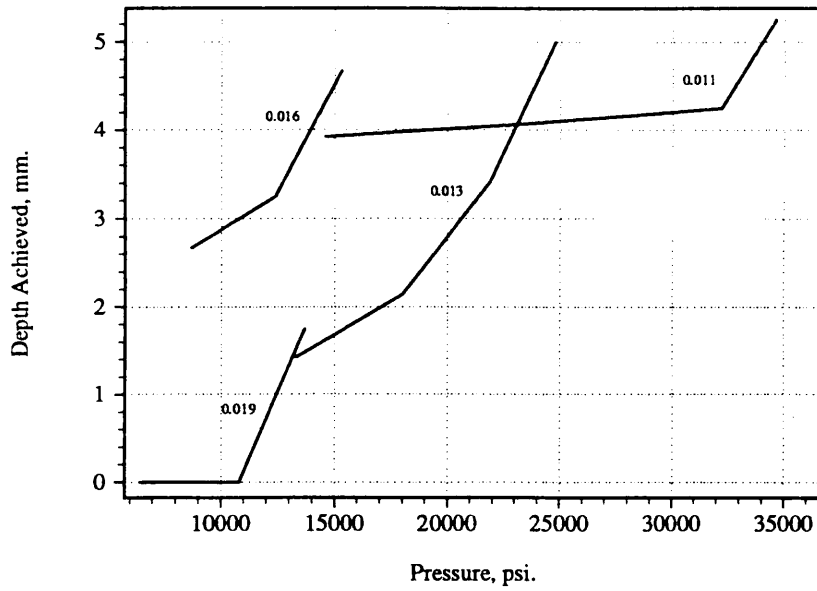
Graph 10.9 Depth Achieved vs. Pressure at Traverse Velocity of 2 in/sec. for Various Nozzle Sizes



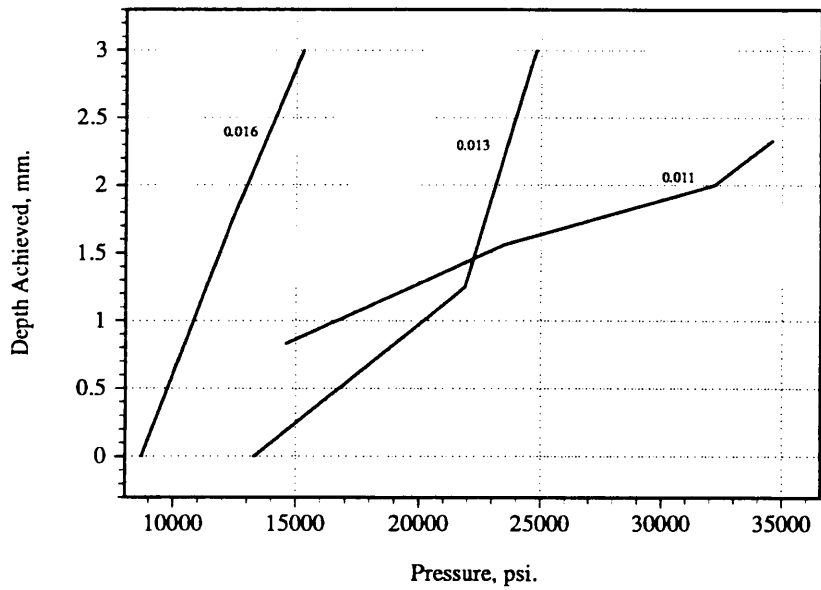
Graph 10.10 Depth Achieved vs. Pressure at Traverse Velocity of 6 in/sec. for Various Nozzle Sizes



Graph 10.11 Depth Achieved vs. Pressure at Traverse Velocity of 12 in/sec. for Various Nozzle Sizes



Graph 10.12 Depth Achieved vs. Pressure at Traverse Velocity of 20 in/sec. for Various Nozzle Sizes



In all the graphs for cutting performance, several basic trends can be seen. At all of the pressure ranges, the driving cutting mechanism was more of a breaking, or spalling, effect than a straight eroding/slotting effect. This accounted for the large volumetric removals in comparison to straight kerfing which would display deep kerfs and low volumetric removal. The cutting mechanism can be attributed to some grain displacement at certain depths, which allowed the water to hydrofracture larger pieces of material towards the free face, thus causing large volumes to be extracted. This is most evident in the smaller nozzle sizes, which could get into the kerf and displace the material. The exception to this was in the test for the width of the kerf where the 0.016 inch nozzle size was large enough to give good point pressure, which concentrated outward instead of downward. It was simply too large to concentrate on deeper hydrofracture.

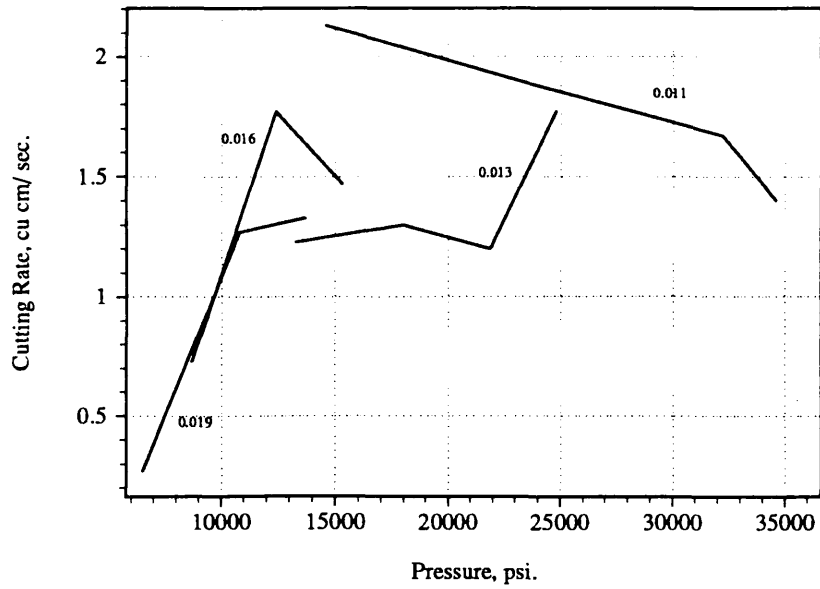
An important aspect of the cutting performance evaluation is the rate of removal. At slower traverse velocities, the volume, depth, and width of the kerf were greatest. But, at larger traverse velocities, the greatest rate of removal was observed. It is better to cut a smaller amount much faster than it is to cut a larger amount much slower.

The effectiveness of trona cutting was measured by the cutting rate achieved, cubic centimeters per second, at various traverse velocities, for a range of nozzle sizes, tested at a range of jet pressures.

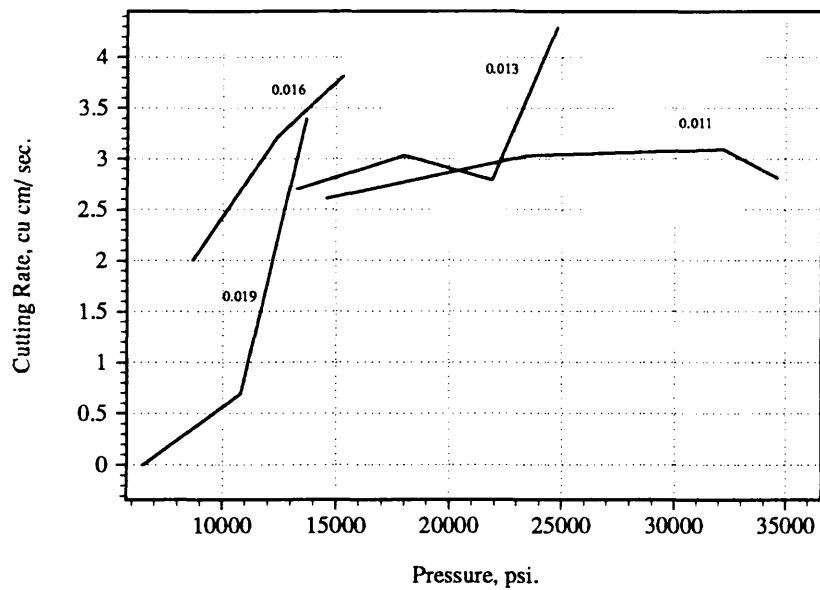
Graphs 10.13, 10.14, 10.15, and 10.16 display the cutting rates achieved, at respective pressures, for each of the traverse velocities, and include all nozzle sizes. The cutting rate was found as the difference between the volumetric removal and the traverse velocity. A general trend was established for all nozzle sizes in terms of the cutting rates achieved at different traverse velocities. In the case

of the smallest three nozzle sizes, the cutting rate increases with an increase of cutting speed, or traverse velocity, from two to 12 inches per second. At the 20 inch per second traverse velocity, the cutting rates drop. This shows that an optimal traverse velocity is approached for cutting rate. The 0.019 inch nozzle size, identified in previous graphs as cutting with a slightly different cutting mechanism, approaches optimal traverse velocity at the six inch per second speed. At the 20 inch per second traverse velocity, this nozzle did not produce any kerf. The highest cutting rate, observed for all nozzle sizes, was found when cutting at 12 inches per second traverse velocity, with the 0.013 inch nozzle size. This rate was observed to be about seven cubic centimeters per second. At this same traverse velocity, the 0.011 inch nozzle size shows very consistent cutting rates, over the entire range of pressures tested. This could be the result of reaching an optimal cutting size in terms of using a lower pressure water jet. All other nozzle sizes appear to increase the cutting rate, with an increase of pressure, for each respective increase of cutting pressure.

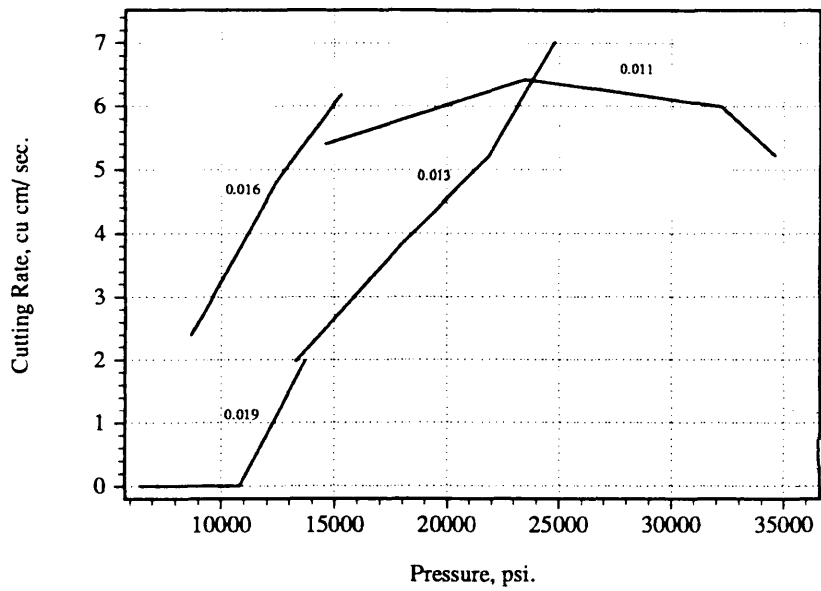
Graph 10.13 Cutting Rate vs. Pressure at Traverse Velocity of 2 in/sec. for Various Nozzle Sizes



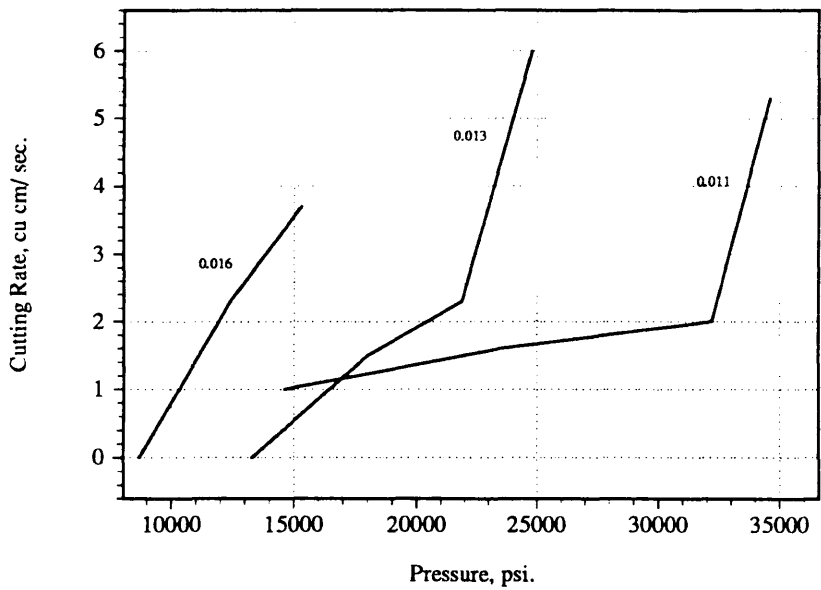
Graph 10.14 Cutting Rate vs. Pressure at Traverse Velocity of 6 in/sec. for Various Nozzle Sizes



Graph 10.15 Cutting Rate vs. Pressure at Traverse Velocity of 12 in/sec. for Various Nozzle Sizes

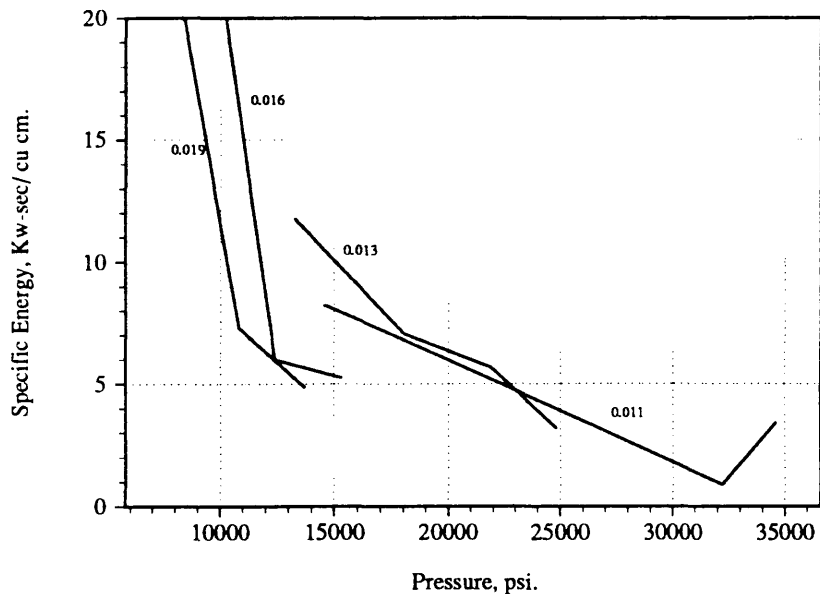


Graph 10.16 Cutting Rate vs. Pressure at Traverse Velocity of 20 in/sec. for Various Nozzle Sizes

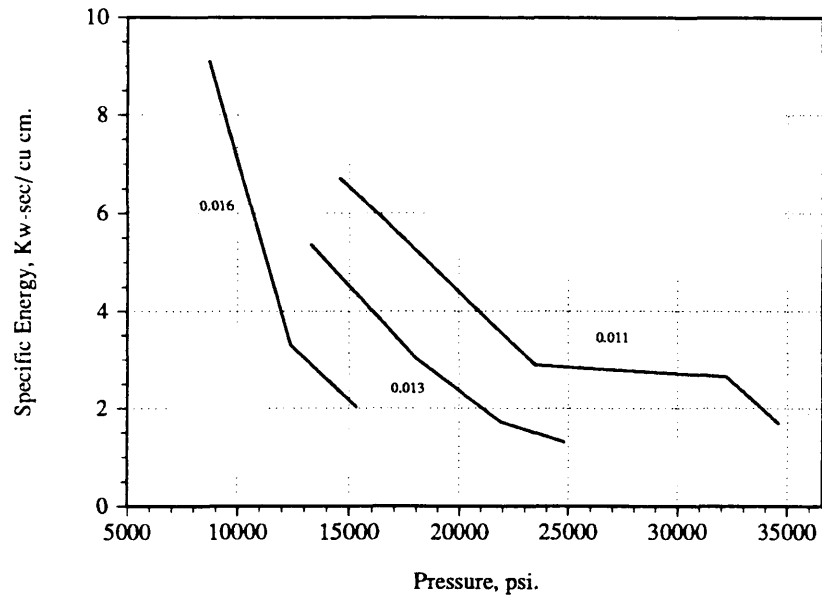


Graphs 10.17, 10.18, 10.19, and 10.20, display the specific energy plotted against the cutting pressure, for each traverse velocity, and include all nozzle sizes. A general trend for all graphs displays a decrease in specific energy, with an increase in pressure. The lowest over all energy consumption per amount of rock removal, was found at the expected 12 inch per second traverse velocity. The larger nozzle sizes are plotted, in all cases, going completely off the graph. In these ranges the nozzles are not producing any appreciable cutting, and therefor, the specific energy is approaching infinity. In the smaller nozzle sizes, the energy is decreasing with increasing pressure. If all nozzle sizes are taken into account, a reverse logarithmic trend can be seen over the range of pressures, for all traverse velocities.

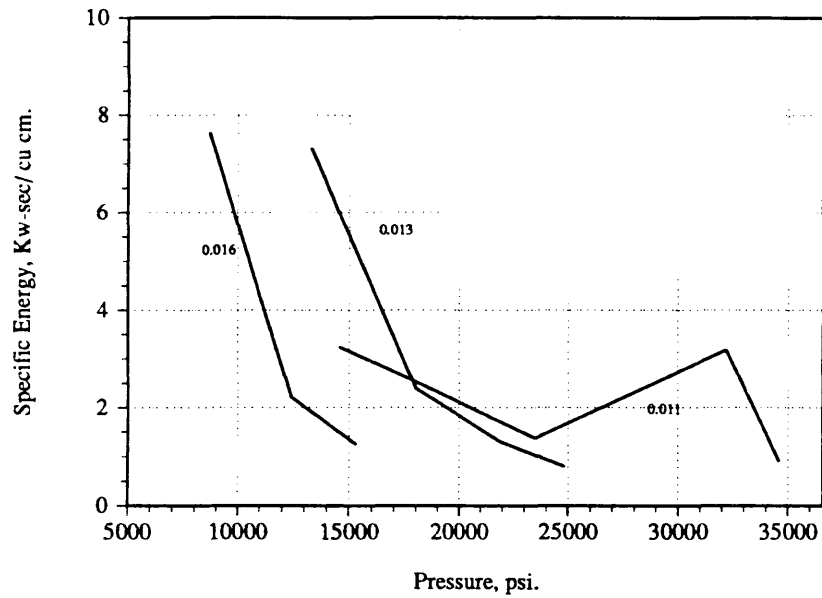
Graph 10.17 Specific Energy vs. Pressure at Traverse Velocity of 2 in/sec. for Various Nozzle Sizes



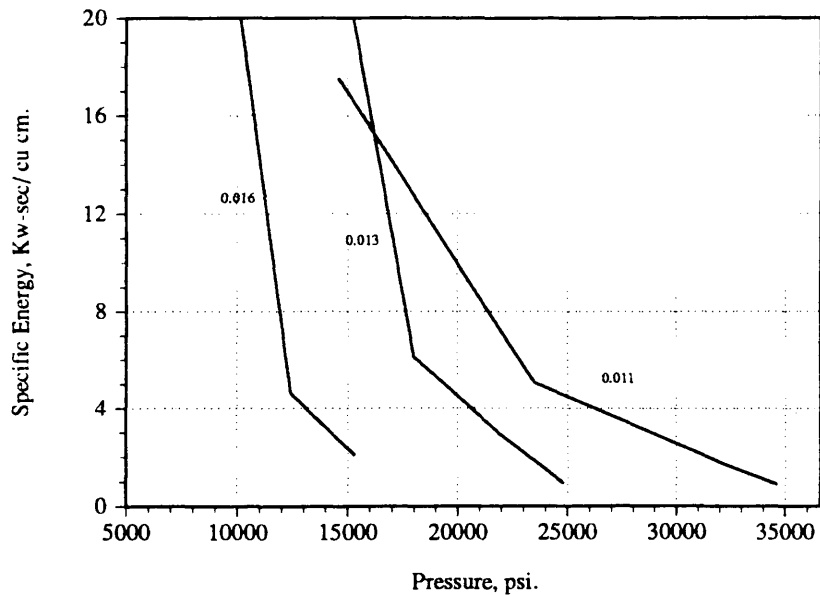
Graph 10.18 Specific Energy vs. Pressure at Traverse Velocity of 6 in/sec. for Various Nozzle Sizes



Graph 10.19 Specific Energy vs. Pressure at Traverse Velocity of 12 in/sec. for Various Nozzle Sizes



Graph 10.20 Specific Energy vs. Pressure at Traverse Velocity of 20 in/sec. for Various Nozzle Sizes



Figures 10.1 through 10.3 are photographs of cut trona samples. Figure 10.1 demonstrates the spalling effect at a slow traverse velocity and a low pressure. Figure 10.2 displays the kerfing effect at a high traverse velocity and lower pressure. Figure 10.3 shows the best result, in terms of rate of removal.

Figures 10.4 and 10.5 are photographs of the water jet test facility and the cutting water jet. In Figure 10.4, the steel table is shown supporting the intensifier pump. The filters are shown below the table surface, and the recharging pump, not seen here, is next to the table. In Figure 10.5, the critical distance of optimal cutting is less than one inch. After this length, the jet tends to fan out, and loose power. The central core is located in the center of the fan of the jet and cannot be seen through the mist.

Figure 10.1 Sample Cut at 2 Inches per Second

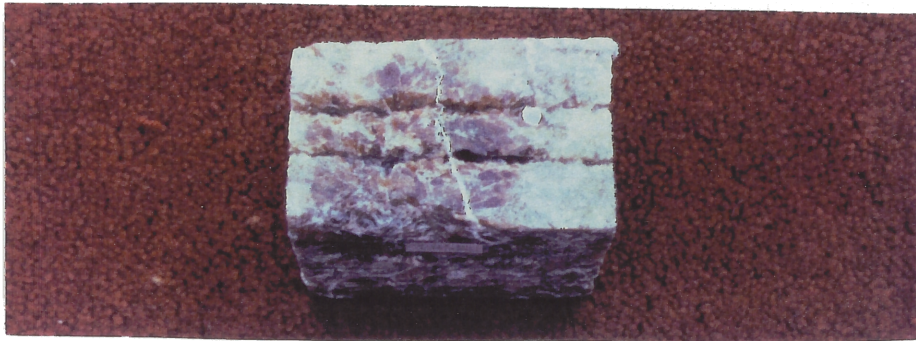


Figure 10.2 Sample Cut at 20 Inches Per Second

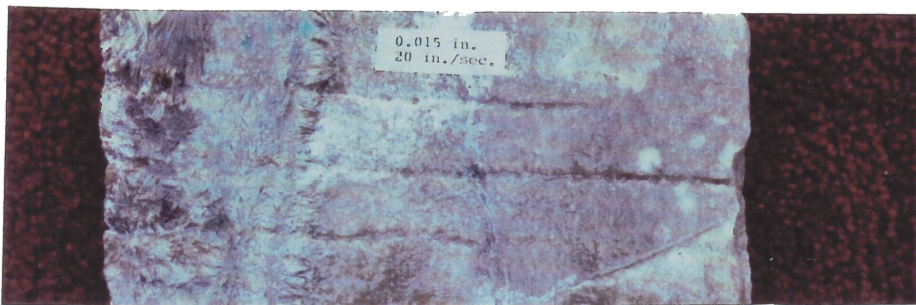


Figure 10.3 Sample Cut at 12 Inches Per Second

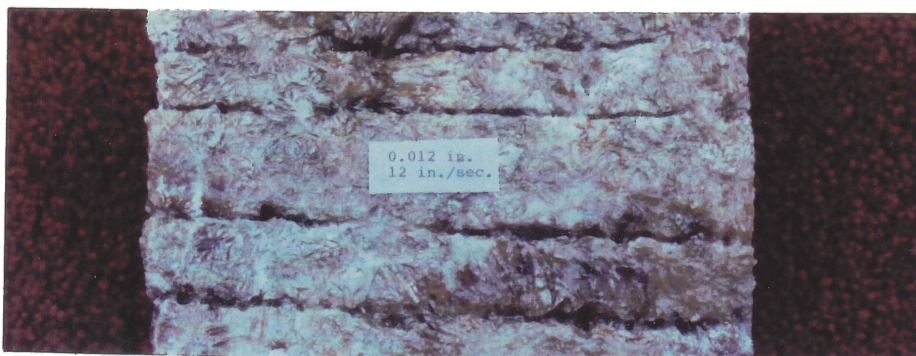


Figure 10.4 Water Jet Test Facility



Figure 10.5 Water Jet at Full Pressure



CHAPTER 11
CONCLUSIONS AND RECOMMENDATIONS

Trona can be cut, to a degree of certainty, with a water jet created by an 8 horsepower pneumatic intensifier pump. This water jet can cut trona within a pressure range of 6,500 to 34,600 psi., and a flow rate of 0.30 to 0.86 gpm. The material properties of trona exhibit radiating crystals imbedded in finer grains. The radiating crystals tend to break free with a spalling effect, and the finer grains are displaced, when the water jet cuts the trona. The most important parameters for trona cutting are the pressure and volume of the water jet, governed by nozzle size and the input driving air pressure.

The effectiveness of trona cutting was determined by the cutting depth, apparent width, volume removed, cutting rate achieved, and the specific energy required to achieve the cutting rate. The most important parameter is the cutting rate, displayed in cubic centimeters per second, at various traverse velocities, for a range of nozzle sizes, tested at a range of jet pressures.

In the original testing procedure, only three nozzle sizes were tested. These were 0.013, 0.016, and 0.019 inches. This was due to the initial calculations performed to determine the nozzle size. After graphing the data, it was found that the results were decreasingly favorable from the 0.013 inch to the 0.019 inch nozzle size. It was determined that a fourth nozzle size, the 0.011 inch size, should be tested to see whether it produced even more favorable results than the 0.013 inch size. If it did, then another nozzle would have been tested until an optimum size was found.

The volumetric removal, for a two inch traverse, in cubic

centimeters at various pressures, was the first parameter addressed in determination of cutting ability for each nozzle size. Graphs were created which correspond to traverse velocities with ranges of two inches per second, six inches per second, 12 inches per second, and 20 inches per second, respectfully.

General trends were established for generalities found in these graphs. Although each nozzle displays different peak pressures, higher volumetric removals are observed at larger pressures up to about 25,000 psi., and then tapering off from there. In general, higher volumetric removals are observed at lower traverse velocities for the range of nozzles tested.

Next, graphs were created to display the apparent kerf width achieved for each traverse velocity, plotted against the range of pressures tested, for each nozzle size. General trends were established in determining the behavior of the water jet, in terms of apparent widths, at various pressures. In the slowest three traverse velocities, kerf width advanced in size up to a pressure of about 15,000 psi., and then tapered off from there. This trend was supported in the literature, as larger pressures are traditionally associated with greater depth, and smaller, or cleaner kerf widths, in a variety of materials. In the case of rock, many tests have found larger kerf widths, associated with larger volumetric removals, at lower pressures. For the data found in this thesis, the smaller nozzle sizes produce larger pressures, and therefor have a trend of decreasing kerf width with increasing pressures. The larger nozzle sizes, on the other hand, tend to increase in kerf width with increasing pressures. This could be associated with the larger jet diameters, which might not produce granular displacement as well as the smaller nozzle sizes. Therefor, the large kerf widths are associated with global fracture based failure, due to micro fracturing

along the crystal boundaries rather than simple individual grain displacement. In support of this argument, the next set of graphs were created to display the kerf depth. It was anticipated that a trend of increasing depth, at higher pressures, would result with decreasing nozzle sizes.

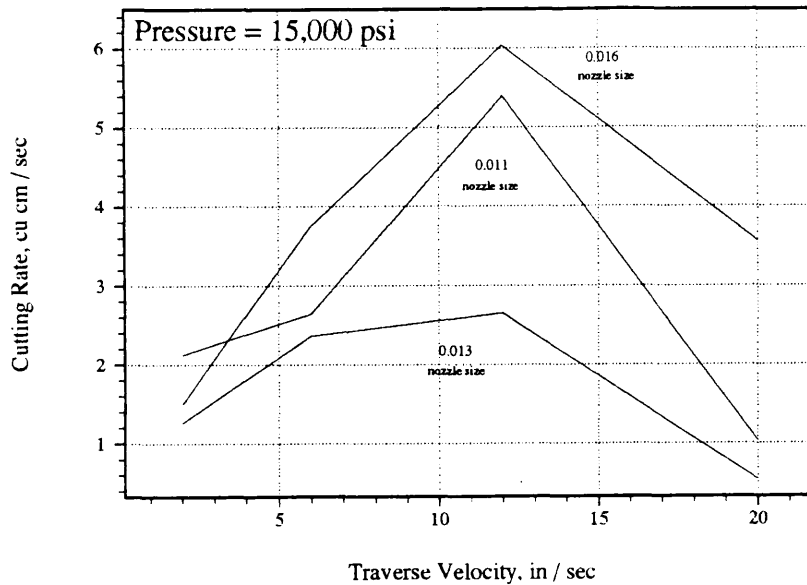
This was indeed the case with the graphs displaying the average kerf depth achieved for each respective traverse velocity, plotted against various pressures, for each nozzle size. A general trend was established for greater depths achieved at greater pressures. All nozzle sizes followed this trend and these graphs displayed this very readily. As traverse velocity increases, the depth achieved tends to decrease. This is expected, as the water jet does not have the same amount of time to act on individual grains, associated with achieving depth. In the literature, all materials tested react similarly to this phenomenon. As pointed out earlier, achievement of depth is not the focus of this thesis, as this does not determine ultimate cutting ability of material in the mining sense. The object of this thesis is to remove material which is a function of depth achieved, width achieved, and ultimately the volume removed in a specific time frame, with a specific amount of energy.

Therefore, the next parameter studied included graphing the rates of removal. At slower traverse velocities, the volume, depth, and width of the kerf were greatest. But, at larger traverse velocities, the greatest rate of removal was observed. It is better to cut a smaller amount much faster than it is to cut a larger amount much slower.

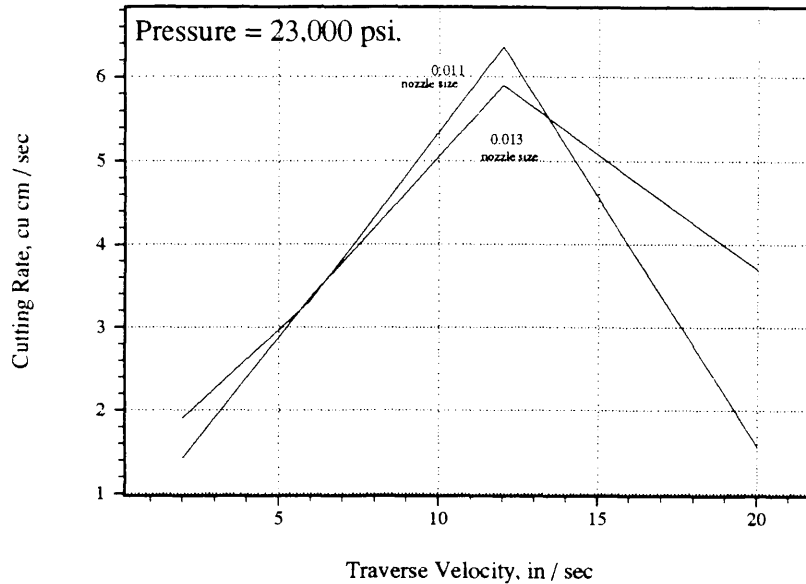
The effectiveness of trona cutting was measured by the cutting rate achieved and specific energy. Graphs were created to display the cutting rates achieved, at respective pressures, for each of the traverse velocities, including all the nozzle sizes. The cutting rate was found by dividing the

volumetric removal with the traverse velocity. A general trend was established for all nozzle sizes in terms of the cutting rates achieved at different traverse velocities, displayed in Graphs 11.1 and 11.2.

Graph 11.1 Traverse Velocity vs. Cutting Rate at Pressure of 15,000 psi.



Graph 11.2 Traverse Velocity vs. Cutting Rate
at Pressure of 23,000 psi.



In the case of the smallest three nozzle sizes, the cutting rate increases with an increase of cutting speed, or traverse velocity, from two to 12 inches per second. At the 20 inch per second traverse velocity, the cutting rates drop. This shows that an optimal traverse velocity is approached for cutting rate. The 0.019 inch nozzle size, identified in previous graphs as cutting with a slightly different cutting mechanism, approaches optimal traverse velocity at the six inch per second speed. At the 20 inch per second traverse velocity, this nozzle did not produce any kerf. The highest cutting rate, observed for all nozzle sizes, was found when cutting at 12 inches per second traverse velocity, with the 0.013 inch nozzle size. This rate was observed to be about seven cubic centimeters per second. At this same traverse velocity, the 0.011 inch nozzle size shows very consistent

cutting rates, over the entire range of pressures tested. This could be the result of reaching an optimal cutting size in terms of using a lower pressure water jet. All other nozzle sizes appear to increase the cutting rate, with an increase of pressure, for each respective increase of cutting pressure.

After finding the optimal cutting rates, graphs were created to display the specific energy plotted against the cutting pressure, for each traverse velocity, for all nozzle sizes. The purpose for these graphs was to compare trends found within the pressure ranges and nozzle sizes, and to compare them with similar water jet tests and conventional mining methods for efficiency. A general trend for all graphs displayed a decrease in specific energy, with an increase in pressure. The lowest over all energy consumption per amount of rock removal, was found at the expected 12 inch per second traverse velocity. The larger nozzle sizes tended to go to infinity at lower pressures. In the smaller nozzle sizes, the energy decreased with increasing pressure. When all nozzle sizes are taken into account, a reverse logarithmic trend can be seen over the range of pressures, for all traverse velocities. This is also the case in all water jet testing previously done by other investigators. When comparing the specific energy requirements of this jet to other methods of rock breakage, the energy appears high at first glance. However, many things are left unaccounted.

Recommendation for further testing is made for several parameters which are not addressed. The spacing of the kerfs, the effect of using multiple passes over existing kerfs, the effect of oscillating the water jet, and the effect of using more powerful jets for cutting trona. Correct spacing of kerfs could produce a greater spalling action. The material between the kerfs might spall toward the free face of existing

kerfs if the spacing is narrow enough for this to occur. If multiple passes are made on existing kerfs, the increased cutting action could cause loose grains and crystals to displace more readily than using only one pass. This could increase the cutting rate, and decrease the specific energy, depending on the number of passes used. Oscillating the water jet can produce a break-up of the jet stream. The trona surface would see this as a form of a pulsing jet with individual pieces of water impacting separately onto free surfaces. This effect could either be used with multiple passes on an existing kerf, or, if the jet is traversed, while oscillating, the effect of kerf spacing could be utilized to cause material fracture toward the free face. The effect of cutting trona with a more powerful water jet would produce greater results.

A more powerful water jet is produced when either the pressure is increased, using the same volume, the volume is increased, using the same pressure, or, both the volume and the pressure are increased. Researching the cutting effect of a water jet, with a pressure up to 50,000 psi., at a volume up to 2 gpm., might display a trona cutting rate many times greater than that found in the scope of this thesis.

REFERENCES CITED

- Bradley, W.H., 1964, "Geology of the Green River Formation and Associated Eocene Rocks in South Western Wyoming and Adjacent Part of Colorado and Utah," Professional Paper 496-A, U.S. Geological Survey.
- Brook, N., and D.A. Summers, 1969, "The Penetration of Rock By High Speed Water Jets," International Journal of Rock Mechanics and Mineral Science, ed.6.
- Chermensky, G.P., 1976, "Breaking Coal and Rock With Pulsed Water Jets," Third Int. Symp. on Jet Cutting Tech., Cranfield, Bedford, England: BHRA Fluid Engineering.
- Conn, A.F., 1976, "Some Basic Fluid Mechanics of Jet Cutting," Introductory Course on Jet Cutting Tech., May 10, Chicago, Cranfield, Bedford, England: BHRA Fluid Engineering.
- Conn, A.F., Cutting by Water Jet: Principles, Systems, Applications, Flow Systems, inc., Kent, WA.
- Cooley, W.C., 1974, "Correlation of Data on Jet Cutting by Water Jets Using Dimensionless Parameters," Second Int. Symp. on Jet Cutting Tech., Cranfield, Bedford, England: BHRA Fluid Engineering.
- Crow, S.C., "A Theory of Hydraulic Rock Cutting," Flow Research Report No. 5, Flow Research, inc., Kent, WA.
- Crow, S.C., P.V. Lade and G.H. Hurlburt, 1974, "The Mechanics of Hydraulic Rock Cutting," Second Int. Symp. on Jet Cutting Tech., Cranfield, Bedford, England: BHRA Fluid Engineering.
- Crow, S.C., 1973, "The Effect of Porosity on Hydraulic Rock Cutting," School of Engineering and Applied Science, University of California, L.A., California.
- Culbertson, W.C., 1965, "Tongues of the Green River and Wasatch Formations in the South Western Part of the Green River Basin, Wyoming," Professional Paper 525-D, U.S. Geologic Survey, pp. D139 - D143.
- Culbertson, W.C., 1966, "Trona in the Wilkins Peak Member of

- the Green River Formation, South Western Wyoming," Professional Paper 550-B, U.S. Geologic Survey, pp. B159 - B164.
- Deardorff, D.L., and L.E. Mannion, 1971, "Wyoming Trona Deposits," Contributions to Geology, Vol. 10, No. 1, R.B. Parker, ed., University of Wyoming, Larimie, pp. 33 - 42
- Farmer, I.W., and P.B. Attwell, 1965, "Rock Penetration by High Velocity Water Jet," International Journal on Rock Mechanics and Mineral Science, Vol. 2, pp. 135 - 153.
- Frank, J.N., D.E. Fogelson and J.W. Chester, 1972, "Hydraulic Mining in the U.S.A.," First Int. Symp. on Jet Cutting Tech., Cranfield, Bedford, England: BHRA Fluid Engineering.
- Haskel, inc., 1989, Haskel Operation and Maintenance Manual for 8-HSFD-225-C Liquid Pump System, Haskel, inc., Burbank, CA.
- Labus, T.J., 1991, Fluid Jet Technology: Fundamentals and Applications, Water Jet Technology Association, inc., St. Louis, MO.
- Leach, S.J., and G.L. Walker, 1966, "Some Aspects of Rock Cutting by High Speed Water Jets," Phil. Trans. R. Soc., A260, pp. 295 - 308.
- McClain, W.C., and G.A. Cristy, 1970, "Examination of High Pressure Water Jets for Use in Rock Tunnel Excavation," Oakridge National Laboratory, Union Carbide Corp., U.S. Atomic Energy Commission, Clearing House for Federal, Scientific, and Technical Information, National Bureau of Standards, U.S. Department of Commerce, Springfield, VA.
- Peele, R., 1927, Mining Engineers' Handbook, Second ed., John Wiley and Sons, Inc., New York, London: Chapman and Hall, Ltd., pp. 898 - 909.
- Summers, D.A., and J.F. Peters, 1974, "The Effect of Rock Anisotropy on the Excavation Rate in Barre Granite," Second Int. Symp. on Jet Cutting Tech., Cranfield, Bedford, England: BHRA Fluid Engineering.
- Summers, D.A., 1983, "Rock and Coal Cutting," The

Application of High Pressure Water Jet Technology, Short Course, University of Missouri Rolla, May 23, Water Jet Technology Association, St. Louis, MO, pp. 103 - 119.

- Tian, B., J. Sun and C. Zou, "Development and Basic Regularities of Water Jet Cutting Technology in China Coal Industry," Department of Mining Mechanical Engineering, China Institute of Mining, Xuzhou City, Jiangsu Province, China.
- Wang, F.D., R. Robbins and J. Olsen, 1976, "Water Jet Assisted Tunnel Boring," Third Int. Symp. on Jet Cutting Tech., ITT Research Institute, BHRA Fluid Engineering.
- Wang, F.D., and J. Wolgamott, 1978, "Application of Water Jet Assisted Pick Cutter for Rock Fragmentation," Fourth Int. Symp. on Jet Cutting Tech., Cranfield, Bedford, England: BHRA Fluid Engineering.
- Wang, F.D., 1984, "Theory and Application of Water Jet in Underground Tunneling," Colorado School of Mines, Golden, CO.
- Wang, F.D., "An Overview of the Application of High Pressure Waterjet Cutting and Cleaning in the Production, Manufacturing, and Service Industries," Colorado School of Mines, Golden, Colorado.
- Zugail, S.A., 1991, "Hydromining Methods: Literature Review," Colorado School of Mines, Golden, CO.

SELECTED BIBLIOGRAPHY

- Bradley, W.H., 1964, "Geology of the Green River Formation and Associated Eocene Rocks in South Western Wyoming and Adjacent Part of Colorado and Utah," Professional Paper 496-A, U.S. Geological Survey.
- Brook, N., and D.A. Summers, 1969, "The Penetration of Rock By High Speed Water Jets," International Journal of Rock Mechanics and Mineral Science, ed.6.
- Chermensky, G.P., 1976, "Breaking Coal and Rock With Pulsed Water Jets," Third Int. Symp. on Jet Cutting Tech., Cranfield, Bedford, England: BHRA Fluid Engineering.
- Conn, A.F., 1976, "Some Basic Fluid Mechanics of Jet Cutting," Introductory Course on Jet Cutting Tech., May 10, Chicago, Cranfield, Bedford, England: BHRA Fluid Engineering.
- Conn, A.F., Cutting by Water Jet: Principles, Systems, Applications, Flow Systems, inc., Kent, WA.
- Cooley, W.C., 1974, "Correlation of Data on Jet Cutting by Water Jets Using Dimensionless Parameters," Second Int. Symp. on Jet Cutting Tech., Cranfield, Bedford, England: BHRA Fluid Engineering.
- Crow, S.C., "A Theory of Hydraulic Rock Cutting," Flow Research Report No. 5, Flow Research, inc., Kent, WA.
- Crow, S.C., P.V. Lade and G.H. Hurlburt, 1974, "The Mechanics of Hydraulic Rock Cutting," Second Int. Symp. on Jet Cutting Tech., Cranfield, Bedford, England: BHRA Fluid Engineering.
- Crow, S.C., 1973, "The Effect of Porosity on Hydraulic Rock Cutting," School of Engineering and Applied Science, University of California, L.A., California.
- Culbertson, W.C., 1965, "Tongues of the Green River and Wasatch Formations in the South Western Part of the Green River Basin, Wyoming," Professional Paper 525-D, U.S. Geologic Survey, pp. D139 - D143.
- Culbertson, W.C., 1966, "Trona in the Wilkins Peak Member of

- the Green River Formation, South Western Wyoming," Professional Paper 550-B, U.S. Geologic Survey, pp. B159 - B164.
- Daniel, I.M., 1974, "Experimental Study of Mechanics of Rock Fracture by Water Jet," ITT Research Institute, Chicago, IL.
- Deardorff, D.L., and L.E. Mannion, 1971, "Wyoming Trona Deposits," Contributions to Geology, Vol. 10, No. 1, R.B. Parker, ed., University of Wyoming, Larimie, pp. 33 - 42
- Dibble, M.F., 1991, "Borehole Mining: Improved Technology Expands Horizon," Mining Engineering, March ed.
- Farmer, I.W., and P.B. Attwell, 1965, "Rock Penetration by High Velocity Water Jet," International Journal on Rock Mechanics and Mineral Science, Vol. 2, pp. 135 - 153.
- Frank, J.N., D.E. Fogelson and J.W. Chester, 1972, "Hydraulic Mining in the U.S.A.," First Int. Symp. on Jet Cutting Tech., Cranfield, Bedford, England: BHRA Fluid Engineering.
- Harris, H.D., and M. Mellor, 1974, "Penetration of Rocks by Continuous Water Jets," Second Int. Symp. on Jet Cutting Tech., Cranfield, Bedford, England: BHRA Fluid Engineering.
- Haskel, inc., 1989, Haskel Operation and Maintenance Manual for 8-HSFD-225-C Liquid Pump System, Haskel, inc., Burbank, CA.
- International Engineering Technology, inc., 1986, "The State-of-the-Art of Hydraulic Mining Practices in China," Denver Mining Research Center, U.S. Bureau of Mines, Denver, CO.
- Labus, T.J., 1976, "High Pressure Water Jet Technology: Principles and Application," ITT Research Institute, Chicago, IL.
- Labus, T.J., 1991, Fluid Jet Technology: Fundamentals and Applications, Water Jet Technology Association, inc., St. Louis, MO.
- Leach, S.J., and G.L. Walker, 1966, "Some Aspects of Rock

- Cutting by High Speed Water Jets," Phil. Trans. R. Soc., A260, pp. 295 - 308.
- McClain, W.C., and G.A. Cristy, 1970, "Examination of High Pressure Water Jets for Use in Rock Tunnel Excavation," Oakridge National Laboratory, Union Carbide Corp., U.S. Atomic Energy Commission, Clearing House for Federal, Scientific, and Technical Information, National Bureau of Standards, U.S. Department of Commerce, Springfield, VA.
- Peele, R., 1927, Mining Engineers' Handbook, Second ed., John Wiley and Sons, Inc., New York, London: Chapman and Hall, Ltd., pp. 898 - 909.
- Pritchett, J.W., and T.D. Riney, "Analysis of Dynamic Stresses Imposed on Rocks by Water Jet Impact," Systems, Science, and Software, La Jolla, CA.
- Rehbinder, G., 1976, "Some Aspects on the Mechanism of Erosion of Rock With a High Speed Water Jet," Third Int. Symp. on Jet Cutting Tech., Cranfield, Bedford, England: BHRA Fluid Engineering.
- Reichman, J.M., 1984, "Optimization of Water Jet Systems for Mining Applications," Bureau of Mines Water Jet Technology Transfer, Flow Industries, inc., Kent, WA.
- Remisz, J.W., 1987, "Jet Cutting of Brown Coal," International Water Jet Symposium, Beijing, China.
- Sato, K., 1987, "Automation of Hydraulic Mining," International Water Jet Symposium, Beijing, China.
- Summers, D.A., and J.F. Peters, 1974, "The Effect of Rock Anisotropy on the Excavation Rate in Barre Granite," Second Int. Symp. on Jet Cutting Tech., Cranfield, Bedford, England: BHRA Fluid Engineering.
- Summers, D.A., 1983, "Rock and Coal Cutting," The Application of High Pressure Water Jet Technology, Short Course, University of Missouri Rolla, May 23, Water Jet Technology Association, St. Louis, MO, pp. 103 - 119.
- Tian, B., J. Sun and C. Zou, "Development and Basic Regularities of Water Jet Cutting Technology in China Coal Industry," Department of Mining Mechanical

Engineering, China Institute of Mining, Xuzhou City, Jiangsu Province, China.

- Wang, F.D., R. Robbins and J. Olsen, 1976, "Water Jet Assisted Tunnel Boring," Third Int. Symp. on Jet Cutting Tech., ITT Research Institute, BHRA Fluid Engineering.
- Wang, F.D., and J. Wolgamott, 1978, "Application of Water Jet Assisted Pick Cutter for Rock Fragmentation," Fourth Int. Symp. on Jet Cutting Tech., Cranfield, Bedford, England: BHRA Fluid Engineering.
- Wang, F.D., 1984, "Theory and Application of Water Jet in Underground Tunneling," Colorado School of Mines, Golden, CO.
- Wang, F.D., "An Overview of the Application of High Pressure Waterjet Cutting and Cleaning in the Production, Manufacturing, and Service Industries," Colorado School of Mines, Golden, Colorado.
- Zugail, S.A., 1991, "Hydromining Methods: Literature Review," Colorado School of Mines, Golden, CO.

APPENDIX

The appendix includes all of the physical data measured directly from each kerf tested. Each data point represents the average data taken from three separate kerfs created with the water jet. Each of the three repetitions, for each data point, was made on separate samples, so as not to bias any one point with the same trona sample.

The data is presented in groups representing three to four data points, over a range of pressures, for specific nozzle sizes and traverse velocities. Each group includes average values for depth, width, and volume of each kerf measured.

Depth measurements were taken on the best two inch stretch identified on each kerf. A total of four measurements were taken using a fine wire and a ruler and these are represented in millimeters. The averages for three trials are shown in the bottom column of each data group for each pressure range. The abbreviation for the depth measurement is Kd.

Width measurements are taken by using the same millimeter rule, on the same identified two inch stretch. For this measurement the smallest and the largest widths occurring are displayed for each kerf. These are averaged and the averages for each of the three trials are placed in the bottom column, denoted total, for each of the pressure ranges tested. The abbreviation for the width measurement is Kw.

Volume measurements are taken by filling the identified two inch section with a putty. The putty is displaced in water in a graduated cylinder. This measurement is taken in the units of cubic centimeters. This value is the amount of

trona removed in cubic centimeters for the identified best two inch stretch of kerf. The averages of the three trials are shown in the bottom column of each data group for each respective pressure used. The abbreviation for the volume used is Kv.

Nozzle Size, in: 0.011

Traverse Velocity, in/sec: 2

Water Pressure in PSI

| | | 34,600 | | 32,200 | | 23,500 | | 14,600 | |
|-------|----|------------|-------|-----------|-------|-----------|-------|-----------|-------|
| | | Data | Avg | Data | Avg | Data | Avg | Data | Avg |
| Trial | Kd | 14,11,8,10 | 10.75 | 13,9,11,9 | 10.50 | 5,8,13,13 | 9.70 | 5,6,8,7 | 6.50 |
| 1 | Kw | 1 - 10 | 5.50 | 1 - 12 | 7.50 | 2 - 10 | 6.00 | 2 - 20 | 11.00 |
| | Kv | 1.0 | 1.00 | 1.1 | 1.10 | 1.75 | 1.75 | 1.8 | 1.80 |
| Trial | Kd | 10,12,8,7 | 9.25 | 7,9,5,5 | 6.50 | 4,5,7,6 | 5.50 | 6,4,7,5 | 5.50 |
| 2 | Kw | 2 - 12 | 7.00 | 4 - 22 | 13.00 | 2 - 12 | 7.00 | 2 - 15 | 8.50 |
| | Kv | 1.5 | 1.50 | 2.2 | 2.20 | 1.9 | 1.90 | 1.6 | 1.60 |
| Trial | Kd | 15,11,6,12 | 11.00 | 8,10,18,6 | 10.50 | 5,10,14,5 | 8.60 | 10,15,5,6 | 9.00 |
| 3 | Kw | 1 - 10 | 6.50 | 3 - 10 | 6.50 | 2 - 18 | 10.00 | 3 - 15 | 9.00 |
| | Kv | 1.7 | 1.70 | 1.7 | 1.70 | 2.0 | 2.00 | 3.0 | 3.00 |
| TOTAL | Kd | | 10.33 | | 9.17 | | 7.94 | | 7.00 |
| | Kw | | 6.33 | | 9.00 | | 7.60 | | 9.50 |
| | Kv | | 1.40 | | 1.67 | | 1.89 | | 2.13 |

Traverse Velocity, in/sec: 6

Water Pressure in PSI

| | | 34,600 | | 32,200 | | 23,500 | | 14,600 | |
|-------|----|---------|------|----------|------|----------|------|---------|------|
| | | Data | Avg | Data | Avg | Data | Avg | Data | Avg |
| Trial | Kd | 5,6,6,4 | 5.25 | 7,7,6,5 | 6.25 | 1,3,9,12 | 6.30 | 2,3,1,1 | 1.75 |
| 1 | Kw | 2 - 10 | 6.00 | 1 - 6 | 3.50 | 2 - 14 | 8.00 | 1 - 10 | 5.50 |
| | Kv | 1.0 | 1.00 | 0.8 | 0.80 | 0.9 | 0.90 | 0.7 | 0.70 |
| Trial | Kd | 7,6,8,6 | 6.75 | 5,10,6,4 | 6.25 | 1,4,5,8 | 4.50 | 1,3,2,1 | 1.75 |
| 2 | Kw | 2 - 10 | 6.00 | 1 - 10 | 5.50 | 1 - 10 | 5.50 | 1 - 15 | 8.00 |
| | Kv | 0.6 | 0.60 | 0.7 | 0.70 | 1.2 | 1.20 | 1.2 | 1.20 |
| Trial | Kd | 4,6,5,5 | 5.00 | 7,5,8,5 | 6.25 | 3,7,9,3 | 5.50 | 4,3,4,1 | 3.00 |
| 3 | Kw | 1 - 5 | 3.00 | 1 - 12 | 6.50 | 1 - 12 | 6.50 | 2 - 14 | 8.00 |
| | Kv | 0.4 | 0.40 | 1.6 | 1.60 | 1.3 | 1.30 | 0.7 | 0.70 |
| TOTAL | Kd | | 5.67 | | 6.25 | | 5.43 | | 2.17 |
| | Kw | | 5.00 | | 5.17 | | 6.67 | | 7.17 |
| | Kv | | 0.67 | | 1.03 | | 1.12 | | 0.87 |

Nozzle Size, in: 0.011

Traverse Velocity, in/sec: 12

Water Pressure in PSI

| | | 34,600 | | 32,200 | | 23,500 | | 14,600 | |
|---------|----|---------|------|---------|------|---------|------|---------|------|
| | | Data | Avg | Data | Avg | Data | Avg | Data | Avg |
| Trial 1 | Kd | 9,6,4,6 | 6.25 | 5,5,3,2 | 3.75 | 6,6,3,5 | 5.00 | 3,4,1,6 | 3.50 |
| | Kw | 2 - 8 | 5.00 | 2 - 8 | 5.00 | 2 - 9 | 3.50 | 2 - 13 | 7.50 |
| | Kv | 0.9 | 0.90 | 1.0 | 1.00 | 1.0 | 1.00 | 0.8 | 0.80 |
| Trial 2 | Kd | 6,6,3,5 | 5.00 | 6,5,5,2 | 4.50 | 1,2,3,1 | 1.75 | 5,4,4,3 | 4.00 |
| | Kw | 2 - 11 | 6.50 | 3 - 5 | 4.00 | 2 - 11 | 6.50 | 3 - 10 | 6.50 |
| | Kv | 1.3 | 1.30 | 0.8 | 0.80 | 1.1 | 1.10 | 1.1 | 1.10 |
| Trial 3 | Kd | 4,5,6,3 | 4.50 | 6,2,5,5 | 4.50 | 2,6,8,6 | 5.50 | 3,4,4,6 | 4.25 |
| | Kw | 1 - 4 | 2.50 | 2 - 8 | 5.00 | 2 - 8 | 5.00 | 1 - 10 | 5.50 |
| | Kv | 0.4 | 0.40 | 1.2 | 1.20 | 1.1 | 1.10 | 0.8 | 0.80 |
| TOTAL | Kd | | 5.25 | | 4.25 | | 4.07 | | 3.92 |
| | Kw | | 4.67 | | 4.67 | | 5.00 | | 6.50 |
| | Kv | | 0.87 | | 1.00 | | 1.07 | | 0.90 |

Traverse Velocity, in/sec: 20

Water Pressure in PSI

| | | 34,600 | | 32,200 | | 23,500 | | 14,600 | |
|---------|----|---------|------|---------|------|---------|------|---------|------|
| | | Data | Avg | Data | Avg | Data | Avg | Data | Avg |
| Trial 1 | Kd | 3,5,1,1 | 2.50 | 2,3,1,1 | 1.75 | 1,2,2,2 | 1.75 | 2,2,1,1 | 1.50 |
| | Kw | 2 - 10 | 6.00 | 1 - 2 | 1.50 | 1 - 2 | 1.50 | 1 - 2 | 1.50 |
| | Kv | 0.5 | 0.50 | 0.1 | 0.10 | 0.2 | 0.20 | 0.2 | 0.20 |
| Trial 2 | Kd | 3,3,1,2 | 2.25 | 1,1,3,1 | 1.50 | 1,1,1,2 | 1.25 | 1,1,1,1 | 1.00 |
| | Kw | 2 - 8 | 5.00 | 1 - 3 | 2.00 | 1 - 2 | 1.50 | 1 - 1 | 1.00 |
| | Kv | 0.6 | 0.60 | 0.3 | 0.20 | 0.2 | 0.20 | 0.1 | 0.10 |
| Trial 3 | Kd | 3,3,1,2 | 2.25 | 3,2,3,3 | 2.75 | 2,2,2,1 | 1.75 | 0 | 0.00 |
| | Kw | 2 - 6 | 4.00 | 1 - 5 | 3.00 | 1 - 2 | 1.50 | 0 | 0.00 |
| | Kv | 0.5 | 0.50 | 0.3 | 0.30 | 0.1 | 0.10 | 0 | 0.00 |
| TOTAL | Kd | | 2.33 | | 2.00 | | 1.56 | | 0.83 |
| | Kw | | 5.00 | | 2.17 | | 1.50 | | 0.83 |
| | Kv | | 0.53 | | 0.20 | | 0.16 | | 0.10 |

Nozzle Size, in: 0.013

Traverse Velocity, in/sec: 2

Water Pressure in PSI

| | | 24,800 | | 21,900 | | 18,000 | | 13,300 | |
|---------|----|-----------|-------|---------|------|---------|------|---------|-------|
| | | Data | Avg | Data | Avg | Data | Avg | Data | Avg |
| Trial 1 | Kd | 13,12,9,7 | 10.25 | 8,7,5,8 | 7.00 | 3,4,4,4 | 3.75 | 8,6,5,6 | 6.25 |
| | Kw | 3 - 15 | 6.00 | 2 - 5 | 3.50 | 4 - 12 | 8.00 | 3 - 15 | 9.00 |
| | Kv | 2.2 | 2.20 | 1.6 | 1.60 | 1.5 | 1.50 | 1.6 | 1.60 |
| Trial 2 | Kd | 7,12,13,6 | 9.50 | 6,7,7,5 | 6.25 | 6,2,5,9 | 6.50 | 4,4,6,7 | 5.25 |
| | Kw | 2 - 10 | 6.00 | 2 - 7 | 4.50 | 2 - 15 | 8.50 | 2 - 12 | 7.00 |
| | Kv | 1.2 | 1.20 | 1.0 | 1.00 | 1.3 | 1.30 | 1.0 | 1.00 |
| Trial 3 | Kd | 10,8,13,7 | 9.50 | 8,4,5,9 | 6.50 | 2,6,8,8 | 6.00 | 4,4,4,3 | 3.75 |
| | Kw | 2 - 10 | 6.00 | 2 - 9 | 5.50 | 2 - 10 | 6.00 | 3 - 20 | 11.50 |
| | Kv | 1.9 | 1.90 | 1.0 | 1.00 | 1.1 | 1.10 | 1.1 | 1.10 |
| TOTAL | Kd | | 9.75 | | 6.58 | | 5.41 | | 5.08 |
| | Kw | | 6.00 | | 4.50 | | 7.50 | | 9.17 |
| | Kv | | 1.77 | | 1.20 | | 1.30 | | 1.23 |

Traverse Velocity, in/sec: 6

Water Pressure in PSI

| | | 24,800 | | 21,900 | | 18,000 | | 13,300 | |
|---------|----|---------|------|---------|------|---------|------|---------|------|
| | | Data | Avg | Data | Avg | Data | Avg | Data | Avg |
| Trial 1 | Kd | 7,3,4,5 | 4.75 | 7,4,7,5 | 5.75 | 3,3,4,1 | 3.00 | 4,5,2,2 | 3.25 |
| | Kw | 3 - 15 | 9.00 | 1 - 6 | 3.50 | 3 - 9 | 6.00 | 2 - 8 | 5.00 |
| | Kv | 1.8 | 1.80 | 1.0 | 0.80 | 1.0 | 1.00 | 1.0 | 1.00 |
| Trial 2 | Kd | 5,5,4,5 | 4.75 | 7,4,3,7 | 5.25 | 2,3,4,5 | 3.50 | 3,1,2,4 | 2.50 |
| | Kw | 2 - 12 | 7.00 | 1 - 6 | 3.50 | 3 - 6 | 4.50 | 1 - 9 | 5.00 |
| | Kv | 1.2 | 1.20 | 1.0 | 1.00 | 1.1 | 1.10 | 0.9 | 0.90 |
| Trial 3 | Kd | 7,4,7,3 | 5.25 | 4,6,3,5 | 4.50 | 4,4,7,3 | 4.50 | 5,2,2,2 | 2.75 |
| | Kw | 2 - 7 | 4.50 | 1 - 5 | 3.00 | 2 - 4 | 3.00 | 1 - 10 | 5.50 |
| | Kv | 1.3 | 1.30 | 1.0 | 1.00 | 0.9 | 0.90 | 0.8 | 0.80 |
| TOTAL | Kd | | 4.92 | | 5.17 | | 3.68 | | 2.83 |
| | Kw | | 6.83 | | 3.33 | | 4.50 | | 5.17 |
| | Kv | | 1.43 | | 0.93 | | 1.01 | | 0.90 |

Nozzle Size, in: 0.013

Traverse Velocity, in/sec: 12

Water Pressure in PSI

| | | 24,800 | | 21,900 | | 18,000 | | 13,300 | |
|-------|----|---------|------|---------|------|---------|------|---------|------|
| | | Data | Avg | Data | Avg | Data | Avg | Data | Avg |
| Trial | Kd | 5,5,7,4 | 5.25 | 4,5,2,5 | 4.25 | 2,3,3,3 | 2.67 | 3,1,1,2 | 1.75 |
| 1 | Kw | 2 - 14 | 8.00 | 3 - 7 | 5.00 | 1 - 4 | 2.50 | 1 - 8 | 4.50 |
| | Kv | 0.9 | 0.90 | 0.9 | 0.90 | 0.7 | 0.70 | 0.4 | 0.40 |
| Trial | Kd | 7,5,5,4 | 5.25 | 6,4,3,3 | 4.00 | 1,2,2,2 | 1.75 | 1,2,1,1 | 1.25 |
| 2 | Kw | 2 - 12 | 7.00 | 1 - 6 | 3.50 | 3 - 9 | 6.00 | 1 - 5 | 3.00 |
| | Kv | 1.1 | 1.10 | 1.0 | 1.00 | 0.6 | 0.60 | 0.3 | 0.30 |
| Trial | Kd | 6,4,3,5 | 4.50 | 3,2,2,1 | 2.00 | 2,1,2,3 | 2.00 | 1,1,2,1 | 1.25 |
| 3 | Kw | 2 - 12 | 7.00 | 1 - 4 | 2.50 | 2 - 5 | 3.50 | 1 - 5 | 3.00 |
| | Kv | 1.5 | 1.50 | 0.7 | 0.70 | 0.6 | 0.60 | 0.3 | 0.30 |
| TOTAL | Kd | | 5.00 | | 3.42 | | 2.14 | | 1.42 |
| | Kw | | 7.33 | | 3.67 | | 4.00 | | 3.50 |
| | Kv | | 1.17 | | 0.87 | | 0.64 | | 0.33 |

Traverse Velocity, in/sec: 20

Water Pressure in PSI

| | | 24,800 | | 21,900 | | 18,000 | | 13,300 | |
|-------|----|---------|------|---------|------|---------|------|--------|------|
| | | Data | Avg | Data | Avg | Data | Avg | Data | Avg |
| Trial | Kd | 5,2,4,1 | 3.00 | 2,1,1,2 | 1.50 | 0 | 0.00 | 0 | 0.00 |
| 1 | Kw | 1 - 11 | 6.00 | 1 - 3 | 2.00 | 0 | 0.00 | 0 | 0.00 |
| | Kv | 0.6 | 0.60 | 0.2 | 0.20 | 0 | 0.00 | 0 | 0.00 |
| Trial | Kd | 4,2,2,3 | 2.75 | 2,1,1,1 | 1.25 | 0,1,1,1 | 0.75 | 0 | 0.00 |
| 2 | Kw | 2 - 5 | 3.50 | 1 - 3 | 2.00 | 1 - 2 | 1.50 | 0 | 0.00 |
| | Kv | 0.4 | 0.40 | 0.2 | 0.30 | 0.1 | 0.10 | 0 | 0.00 |
| Trial | Kd | 5,5,2,1 | 3.25 | 1,1,1,1 | 1.00 | 0,0,1,1 | 0.50 | 0 | 0.00 |
| 3 | Kw | 3 - 10 | 6.50 | 1 - 2 | 1.50 | 1 - 1 | 1.00 | 0 | 0.00 |
| | Kv | 0.8 | 0.80 | 0.2 | 0.20 | 0.2 | 0.20 | 0 | 0.00 |
| TOTAL | Kd | | 3.00 | | 1.25 | | 0.68 | | 0.00 |
| | Kw | | 5.33 | | 1.83 | | 1.25 | | 0.00 |
| | Kv | | 0.60 | | 0.23 | | 0.15 | | 0.00 |

Nozzle Size, in: 0.016

Traverse Velocity, in/sec: 2

Water Pressure in PSI

| | | 15,300 | | 12,400 | | 8,700 | |
|---------|----|-----------|------|----------|-------|---------|------|
| | | Data | Avg | Data | Avg | Data | Avg |
| Trial 1 | Kd | 5,4,10,12 | 7.75 | 5,2,11,5 | 5.75 | 7,5,3,3 | 4.50 |
| | Kw | 2 - 15 | 8.50 | 2 - 25 | 13.50 | 2 - 12 | 7.00 |
| | Kv | 1.7 | 1.70 | 1.9 | 1.90 | 0.8 | 0.80 |
| Trial 2 | Kd | 5,6,12,6 | 7.25 | 2,4,10,7 | 5.75 | 2,3,7,4 | 4.00 |
| | Kw | 2 - 10 | 6.00 | 2 - 20 | 11.00 | 2 - 12 | 7.00 |
| | Kv | 1.3 | 1.30 | 2.2 | 2.20 | 0.8 | 0.80 |
| Trial 3 | Kd | 6,10,6,5 | 6.75 | 5,3,10,5 | 5.75 | 3,2,6,5 | 3.75 |
| | Kw | 2 - 15 | 8.50 | 2 - 10 | 6.00 | 2 - 12 | 7.00 |
| | Kv | 1.4 | 1.40 | 1.2 | 1.20 | 0.6 | 0.60 |
| TOTAL | Kd | | 7.25 | | 5.75 | | 4.08 |
| | Kw | | 7.67 | | 10.17 | | 7.00 |
| | Kv | | 1.47 | | 1.77 | | 0.73 |

Traverse Velocity, in/sec: 6

Water Pressure in PSI

| | | 15,300 | | 12,400 | | 8,700 | |
|---------|----|---------|-------|---------|------|---------|------|
| | | Data | Avg | Data | Avg | Data | Avg |
| Trial 1 | Kd | 8,7,5,6 | 6.50 | 7,3,2,3 | 3.75 | 4,3,4,2 | 3.25 |
| | Kw | 2 - 7 | 4.50 | 3 - 13 | 8.00 | 2 - 16 | 9.00 |
| | Kv | 1.1 | 1.10 | 1.4 | 1.40 | 0.8 | 0.80 |
| Trial 2 | Kd | 6,5,5,4 | 5.00 | 4,2,3,3 | 3.00 | 2,3,4,2 | 3.50 |
| | Kw | 2 - 10 | 6.00 | 3 - 11 | 5.00 | 2 - 11 | 6.50 |
| | Kv | 1.0 | 1.00 | 0.8 | 0.80 | 0.8 | 0.80 |
| Trial 3 | Kd | 4,5,7,8 | 6.00 | 5,2,7,2 | 4.00 | 2,2,3,1 | 2.00 |
| | Kw | 2 - 20 | 11.00 | 3 - 10 | 6.50 | 1 - 5 | 3.00 |
| | Kv | 1.7 | 1.70 | 1.0 | 1.00 | 0.4 | 0.40 |
| TOTAL | Kd | | 5.83 | | 3.58 | | 2.92 |
| | Kw | | 7.17 | | 6.50 | | 6.17 |
| | Kv | | 1.27 | | 1.07 | | 0.67 |

Nozzle Size, in: 0.016

Traverse Velocity, in/sec: 12

Water Pressure in PSI

| | | 15,300 | | 12,400 | | 8,700 | |
|-------|----|---------|------|---------|------|---------|------|
| | | Data | Avg | Data | Avg | Data | Avg |
| Trial | Kd | 4,4,5,5 | 4.50 | 3,5,3,2 | 3.25 | 4,3,4,1 | 3.00 |
| 1 | Kw | 2 - 8 | 5.00 | 3 - 10 | 6.50 | 2 - 6 | 4.00 |
| | Kv | 0.9 | 0.90 | 0.7 | 0.70 | 0.4 | 0.40 |
| Trial | Kd | 6,5,3,4 | 4.5 | 5,4,3,4 | 4.00 | 1,2,3,5 | 2.75 |
| 2 | Kw | 3 - 15 | 9.00 | 3 - 12 | 7.50 | 2 - 7 | 4.50 |
| | Kv | 1.2 | 1.20 | 0.8 | 0.80 | 0.5 | 0.50 |
| Trial | Kd | 4,3,7,6 | 5.00 | 3,2,3,2 | 2.50 | 4,2,1,2 | 2.25 |
| 3 | Kw | 3 - 10 | 6.5 | 3 - 10 | 6.50 | 2 - 5 | 3.50 |
| | Kv | 1.0 | 1.00 | 0.9 | 0.90 | 0.3 | 0.30 |
| TOTAL | Kd | | 4.67 | | 3.25 | | 2.67 |
| | Kw | | 6.83 | | 6.83 | | 4.00 |
| | Kv | | 1.03 | | 0.80 | | 0.40 |

Traverse Velocity, in/sec: 20

Water Pressure in PSI

| | | 15,300 | | 12,400 | | 8,700 | |
|-------|----|---------|------|---------|------|-------|------|
| | | Data | Avg | Data | Avg | Data | Avg |
| Trial | Kd | 2,2,5,6 | 3.75 | 2,3,1,2 | 2.00 | 0 | 0.00 |
| 1 | Kw | 1 - 10 | 5.50 | 1 - 7 | 4.00 | 0 | 0.00 |
| | Kv | 0.4 | 0.40 | 0.2 | 0.20 | 0 | 0.00 |
| Trial | Kd | 5,1,2,4 | 3.00 | 2,3,1,1 | 1.75 | 0 | 0.00 |
| 2 | Kw | 1 - 12 | 6.50 | 1 - 5 | 3.00 | 0 | 0.00 |
| | Kv | 0.3 | 0.30 | 0.3 | 0.30 | 0 | 0.00 |
| Trial | Kd | 5,2,1,1 | 2.25 | 1,2,1,2 | 1.50 | 0 | 0.00 |
| 3 | Kw | 1 - 14 | 7.50 | 1 - 4 | 2.50 | 0 | 0.00 |
| | Kv | 0.4 | 0.40 | 0.2 | 0.20 | 0 | 0.00 |
| TOTAL | Kd | | 3.00 | | 1.75 | | 0.00 |
| | Kw | | 6.50 | | 3.17 | | 0.00 |
| | Kv | | 0.37 | | 0.23 | | 0.00 |

Nozzle Size, in: 0.019

Traverse Velocity, in/sec: 2

Water Pressure in PSI

| | | 13,700 | | 10,800 | | 6,500 | |
|-------|----|-----------|------|-----------|------|---------|------|
| | | Data | Avg | Data | Avg | Data | Avg |
| Trial | Kd | 5,4,7,14 | 7.50 | 7,3,2,12 | 5.75 | 2,1,1,1 | 1.25 |
| 1 | Kw | 4 - 10 | 7.00 | 3 - 7 | 5.00 | 2 - 5 | 3.50 |
| | Kv | 1.2 | 1.20 | 1.4 | 1.40 | 0.2 | 0.20 |
| Trial | Kd | 13,10,4,5 | 8.00 | 2,4,7,5 | 4.50 | 3,2,4,1 | 2.50 |
| 2 | Kw | 4 - 10 | 7.00 | 3 - 9 | 6.00 | 2 - 4 | 3.00 |
| | Kv | 1.8 | 1.80 | 1.4 | 1.40 | 0.3 | 0.30 |
| Trial | Kd | 6,3,4,5 | 4.50 | 7,4,10,11 | 8.00 | 2,2,3,1 | 2.00 |
| 3 | Kw | 3 - 8 | 5.50 | 3 - 8 | 5.50 | 2 - 3 | 2.50 |
| | Kv | 1.0 | 1.00 | 1.0 | 1.00 | 0.3 | 0.30 |
| TOTAL | Kd | | 6.67 | | 6.08 | | 1.92 |
| | Kw | | 6.50 | | 5.50 | | 3.00 |
| | Kv | | 1.33 | | 1.27 | | 0.27 |

Traverse Velocity, in/sec: 6

Water Pressure in PSI

| | | 13,700 | | 10,800 | | 6,500 | |
|-------|----|---------|------|---------|------|-------|------|
| | | Data | Avg | Data | Avg | Data | Avg |
| Trial | Kd | 6,5,4,3 | 4.50 | 2,2,1,1 | 1.50 | 0 | 0.00 |
| 1 | Kw | 5 - 10 | 7.50 | 0 - 6 | 3.00 | 0 | 0.00 |
| | Kv | 1.0 | 1.00 | 0.3 | 0.30 | 0 | 0.00 |
| Trial | Kd | 8,3,5,5 | 5.25 | 1,2,1,1 | 1.25 | 0 | 0.00 |
| 2 | Kw | 5 - 10 | 7.50 | 0 - 5 | 2.50 | 0 | 0.00 |
| | Kv | 1.3 | 1.30 | 0.2 | 0.20 | 0 | 0.00 |
| Trial | Kd | 3,7,5,4 | 4.75 | 1,1,1,2 | 1.25 | 0 | 0.00 |
| 3 | Kw | 3 - 6 | 4.50 | 0 - 3 | 1.50 | 0 | 0.00 |
| | Kv | 1.1 | 1.10 | 0.2 | 0.20 | 0 | 0.00 |
| TOTAL | Kd | | 4.83 | | 1.33 | | 0.00 |
| | Kw | | 6.50 | | 2.33 | | 0.00 |
| | Kv | | 1.13 | | 0.23 | | 0.00 |

Nozzle Size, in: 0.019

Traverse Velocity, in/sec: 12

Water Pressure in PSI

| | | 13,700 | | 10,800 | | 6,500 | |
|-------|----|---------|------|--------|------|-------|------|
| | | Data | Avg | Data | Avg | Data | Avg |
| Trial | Kd | 4,1,1,1 | 1.75 | 0 | 0.00 | 0 | 0.00 |
| 1 | Kw | 0 - 5 | 2.50 | 0 | 0.00 | 0 | 0.00 |
| | Kv | 0.3 | 0.30 | 0 | 0.00 | 0 | 0.00 |
| Trial | Kd | 3,1,2,1 | 1.75 | 0 | 0.00 | 0 | 0.00 |
| 2 | Kw | 0 - 12 | 6.00 | 0 | 0.00 | 0 | 0.00 |
| | Kv | 0.4 | 0.40 | 0 | 0.00 | 0 | 0.00 |
| Trial | Kd | 2,3,1,1 | 1.75 | 0 | 0.00 | 0 | 0.00 |
| 3 | Kw | 0 - 5 | 2.50 | 0 | 0.00 | 0 | 0.00 |
| | Kv | 0.3 | 0.30 | 0 | 0.00 | 0 | 0.00 |
| TOTAL | Kd | | 1.75 | | 0.00 | | 0.00 |
| | Kw | | 3.67 | | 0.00 | | 0.00 |
| | Kv | | 0.33 | | 0.00 | | 0.00 |

Traverse Velocity, in/sec: 20

Water Pressure in PSI

| | | 13,700 | | 10,800 | | 6,500 | |
|-------|----|--------|------|--------|------|-------|------|
| | | Data | Avg | Data | Avg | Data | Avg |
| Trial | Kd | 0 | 0.00 | 0 | 0.00 | 0 | 0.00 |
| 1 | Kw | 0 | 0.00 | 0 | 0.00 | 0 | 0.00 |
| | Kv | 0 | 0.00 | 0 | 0.00 | 0 | 0.00 |
| Trial | Kd | 0 | 0.00 | 0 | 0.00 | 0 | 0.00 |
| 2 | Kw | 0 | 0.00 | 0 | 0.00 | 0 | 0.00 |
| | Kv | 0 | 0.00 | 0 | 0.00 | 0 | 0.00 |
| Trial | Kd | 0 | 0.00 | 0 | 0.00 | 0 | 0.00 |
| 3 | Kw | 0 | 0.00 | 0 | 0.00 | 0 | 0.00 |
| | Kv | 0 | 0.00 | 0 | 0.00 | 0 | 0.00 |
| TOTAL | Kd | | 0.00 | | 0.00 | | 0.00 |
| | Kw | | 0.00 | | 0.00 | | 0.00 |
| | Kv | | 0.00 | | 0.00 | | 0.00 |